Centrosome-, mitotic spindle- and cytokinetic bridge-specific compartmentalization of AGO2 protein in human liver cells undergoing mitosis: Non-canonical, RNAi-dependent, control of local homeostasis

ELENI I. THEOTOKI[1,2], PANOS KAKOULIDIS[2,3], KONSTANTINOS-STYLIANOS NIKOLAKOPOULOS[1], ELENI N. VLACHOU[1], OURANIA E. TSITSILONIS[4], GERASSIMOS E. VOUTSINAS[5], EMA ANASTASIADOU[2,6*] and DIMITRIOS J. STRAVOPODIS[1*]

[1]Section of Cell Biology and Biophysics, Department of Biology, School of Science, National and Kapodistrian University of Athens, Athens 15701, Greece; [2]Department of Cancer Genetics, Center of Basic Research, Biomedical Research Foundation of The Academy of Athens, Athens 11527, Greece; [3]Department of Informatics and Telecommunications, School of Science, National and Kapodistrian University of Athens, Athens 15701, Greece; [4]Section of Animal and Human Physiology, Department of Biology, School of Science, National and Kapodistrian University of Athens, Athens 15701, Greece; [5]Laboratory of Molecular Carcinogenesis and Rare Disease Genetics, Institute of Biosciences and Applications, National Center for Scientific Research 'Demokritos', Athens 15310, Greece; [6]Department of Health Science, Higher Colleges of Technology, Dubai 17155, United Arab Emirates

Received March 31, 2025; Accepted June 13, 2025

DOI: 10.3892/mmr.2025.13609

Abstract. Argonaute RNA-induced silencing complex catalytic component 2 (AGO2) is an evolutionary conserved protein involved in microRNA-dependent gene expression regulation via the RNA interference (RNAi) mechanism. Nevertheless, AGO2 may also be involved in other key processes, such as histone modification, DNA methylation and alternative splicing. Its role in the proper development of organisms is key and no homologue is able to compensate for its loss. Therefore, using advanced immunofluorescence, transient transfection and molecular bioinformatics, the present study aimed to investigate novel, non-canonical, RNAi-dependent functions of AGO2 protein in mRNA/protein local homeostasis. The data revealed microtubule network-dependent, localization of AGO2 in both centrosome and mitotic spindle assemblies during cell division and in the cytokinetic bridge formed during the last stage of mitosis (cytokinesis). Detection of AGO2 protein in these mitosis-specific compartments, regardless of the presence of malignant phenotypes or multiple centrosomes/mitotic spindles in liver cells, indicates the cardinal role of AGO2 in centrosome biosynthesis, mitotic spindle formation and function, potentially controlling locality-dependent homeostasis, in a novel non-canonical, RNAi-dependent manner. This novel AGO2/centrosome/mitotic spindle/cytokinetic bridge pathway may serve as a versatile molecular 'toolbox' for targeted therapy of human malignancy, including liver cancer.

Correspondence to: Dr Ema Anastasiadou, Department of Health Science, Higher Colleges of Technology, Academic City Campus, Dubai 17155, United Arab Emirates
E-mail: eanastasiadou@hct.ac.ae

Professor Dimitrios J. Stravopodis, Section of Cell Biology and Biophysics, Department of Biology, School of Science, National and Kapodistrian University of Athens, Athens 15701, Greece
E-mail: dstravop@biol.uoa.gr

*Contributed equally

Key words: argonaute2, centrosome, cytokinetic bridge, HepG2, LX-2, mitotic spindle, RNA interference

Introduction

MicroRNAs (miRNAs) are endogenous, non-coding, single stranded RNAs, with a size of 19-25 nucleotides, involved in RNA interference (RNAi), which can direct post-transcriptional suppression via complementarity to selected mRNA transcripts (1-3). Because of their role as negative regulators of gene expression, miRNAs are essential for proper function and development of an organism. miRNAs regulate >30% of mRNAs, serving key roles in diverse cellular processes, such as differentiation, cell proliferation, stress response and apoptosis (2,4,5), and in mechanisms associated with neuro-development (6,7) and organogenesis (8). Argonaute (AGO) proteins form the core of the RNA-induced silencing complex (RISC) and interact directly with miRNAs (9-11). Specifically, generated miRNAs are loaded as duplexes, containing functional guide and passenger strands, onto the AGOs, a process that is typically followed by the unwinding of double-stranded RNA (12,13). Subsequently, the mature miRNA guides RISC to complementary mRNA targets,

causing downregulation of their expression, through either mRNA cleavage or translational suppression, depending on whether the miRNA has full or partial complementarity to its target mRNA, respectively (4,14-16).

AGOs constitute evolutionary conserved proteins that are ubiquitously expressed in all tissue (17-19). In humans, the AGO family includes four members: AGO1, AGO2, AGO3 and AGO4, which share an ~80% amino acid identity (17,20). Typically, each AGO protein consists of four primary domains that are called (ordered from N- to C-terminus) 'N', 'PAZ', 'MID' and 'PIWI' domain, and connected by two linker domains, 'L1' and 'L2', creating a 'Y'-shaped RNA-binding channel bifurcated by the N domain (20,21). N domain serves the loading of miRNAs onto AGOs, while PAZ and MID domains recognize the 5' and 3' ends of the guide RNA strand, respectively. The PIWI domain structurally resembles RNase H and, thus, is responsible for target cleavage. The L1 and L2 linkers are located between the N and PAZ, and the PAZ and MID domains, respectively, serving a structural rather than functional role (9,21-24).

Due to similarities in molecular structures, the four AGO paralogs are hypothesized to carry out largely overlapping functions. However, each AGO protein serves distinct roles that mainly depend on the cell type, or specific cellular setting and environment. AGO2 is the most extensively studied protein of the family, since it is the only member with catalytic activity and serves an essential role in RISC function, although, AGO3 has also been revealed to be catalytically activated by shorter miRNA species (25-27). The human *AGO2* gene (*HAGO2*) is located on chromosome 8 and its product, the AGO2 protein, resides predominantly in the cytoplasm, where it serves its primary role in gene expression regulation via key engagement in the RNAi mechanism (28,29). However, a number of studies have described AGO2 distribution in the nucleus, where it controls histone modification, DNA methylation and alternative splicing processes (18,30,31). AGO2 is key for mouse development, with its loss causing embryonic lethality early in development, and its activity controlling the early development of lymphoid and erythroid cells (32-35).

Given its intracellular topology in the cytoplasm or/and in the nucleus, the present study aimed to investigate AGO2's compartmentalization in critical cell organelles and assemblies, during mitosis, seeking to discover new roles of AGO2 in spatiotemporal homeostasis control.

Materials and methods

Cell culture. Human cell lines LX-2 (stellate liver cells; cat. no. SCC064; MilliporeSigma) and HepG2 (liver cancer cells; American Type Culture Collection; cat. no. HB-8065; LGC Limited) were cultured in standard conditions (37˚C and 5% CO_2), using 1X DMEM (cat. no. 41966-029), supplemented with 10% FBS (cat. no. 16000044), 1% penicillin/streptomycin (cat. no. 10378016; all Gibco; Thermo Fisher Scientific, Inc.) and 1% L-Glutamine (cat. no. BEBP17-605E; Lonza Group, Ltd.). Both LX-2 and HepG2 cell lines have been authenticated by advanced transcriptomics, proteomics, metabolomics and functional kinomics (whole-kinome activity) profiling.

Transfection. LX-2 cells ($6x10^4$; ~80% confluency) were transiently transfected with the expression plasmids EGFP-hAgo2 (cat. no. 21981; 0.8 μg) and RNT1-GFP (cat. no. 17708; both Addgene, Inc.) (0.8 μg), using Lipofectamine® 2000 (cat. no. 11668027; Invitrogen; Thermo Fisher Scientific, Inc.; 1.5 μl), according to manufacturer's instructions for 6 h at 37˚C. The pcDNA3.1(+) (cat. no. V790-20; Addgene, Inc.) empty vector served as a negative control. Cells were incubated at 37˚C and 5% CO_2, for 24 h post-transfection for immunofluorescence.

Immunofluorescence. LX-2 and HepG2 cells ($6x10^4$; ~80% confluency) were cultured on 10 mm round coverslips and fixed in 4% paraformaldehyde (cat. no. P6148; Merck KGaA) solution for 10 min at room temperature. The cells were membrane-permeabilized by incubation in 0.1% Triton-X 100 (cat. no. 1086031000; Merck KGaA), followed by blocking with 5% BSA (cat. no. A7906; Merck KGaA) for 1 h at room temperature. Cells were exposed to anti-AGO2 (cat. no. ab57113; Abcam) (1:100), anti-DICER (double-stranded RNA endoribonuclease) (cat. no. NBP1-06520; Novus Biologicals, LLC) (1:100), anti-TRBP (transactivation response element RNA-binding protein; cat. no. ab180947; Abcam) (1:100), anti-UPF1 (up-frameshift protein 1) (cat. no. 12040, Cell Signalling Technology, Inc.; 1:100), anti-centrin-2 (cat. no. 2091, Cell Signalling Technology, Inc.) (1:200), anti-peri-centriolar-material (PCM)-1 (cat. no. 5213, Cell Signalling Technology, Inc) (1:200), anti-γ-tubulin (cat. no. T5192; Merck KGaA) (1:200) and anti-α-tubulin (cat. no. 3873, Cell Signalling Technology, Inc.) (1:100) primary antibodies, overnight at 4˚C. Cells were incubated with secondary antibodies [goat anti-mouse (cat. no. A-11004; Invitrogen; Thermo Fisher Scientific, Inc.) and anti-rabbit IgG (H+L)-Alexa Fluor™ 568 (cat. no. A-11011; Invitrogen, Thermo Fisher Scientific, Inc.) and anti-mouse IgG (H+L)-Alexa Fluor 488 (cat. no. A-28175; Invitrogen; Thermo Fisher Scientific, Inc.) and donkey anti-rabbit IgG (H+L)-Alexa Fluor 488 (cat. no. A-21206, Invitrogen; Thermo Fisher Scientific, Inc.)] (1:500) for 1 h at room temperature. Vectashield® Mounting Medium, with DAPI (Vector Laboratories, Inc.), was used to visualize cell nuclei at 405 nm excitation wavelength, using confocal laser scanning microscopy.

Drug treatment. LX-2 cells ($6x10^4$; ~80% confluency) were treated with 0.4 μg/μl demecolcine (cat. no. D7385; Merck KGaA), an inhibitor of tubulin polymerization, for 6 h at 37˚C, and processed (fixation in 4% paraformaldehyde solution for 10 min at room temperature, followed by blocking in 5% BSA for 1 h at room temperature) for immunofluorescence. DMSO (cat. no. A3672; Merck KGaA) was used as the control (reference condition).

Confocal laser scanning microscopy. Observation of immunofluorescence stained, or transiently transfected fluorescent cells was performed using the Confocal Laser Scanning Microscope Leica SP5 (Leica Microsystems GmbH) and LAS-AF (version 2.7.3.9723) software (Leica Microsystems GmbH).

Molecular modelling. For modelling, the experimental structure with the highest resolution available was selected for AGO2 [Protein Databank (PDB) ID: 4Z4D chain: A (4Z4D.A)] (36).

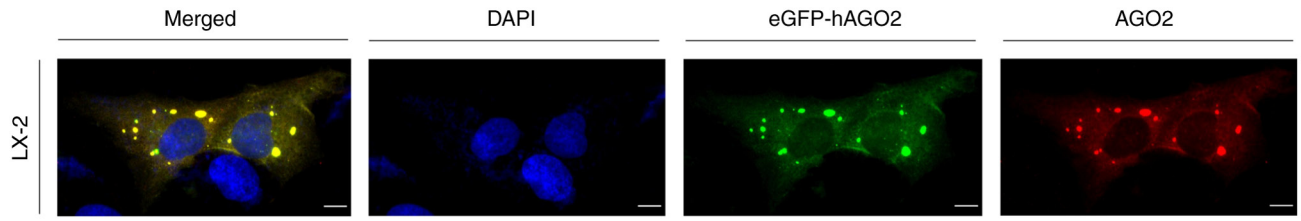

Figure 1. Punctuate patterning of AGO2 protein in the cytoplasm of LX-2 liver cells during interphase. Confocal laser scanning immunofluorescence images of LX-2 cells at the interphase stage overexpressing the human AGO2 protein being fused with the GFP reporter protein (eGFP-hAGO2), after immuno-staining with an anti-AGO2 primary antibody. Overlap (yellow) demonstrated the specificity of the anti-AGO2 primary antibody. Nuclei were visualized with DAPI staining (blue). Scale bar, 10 μm. AGO2, argonaute RNA-induced silencing complex catalytic component 2.

Structure was retrieved from PDB-REDO (37) and refined using the Protein Preparation Wizard of the Schrödinger Maestro Suite (version 2023-2) (38). The ClusPro Server (39) was used to predict docking positions for AGO2-UPF1 (PDB ID: 6EJ5.A) (40) and AGO2-centrin-2 (PDB ID: 8EBX.J) (41). Constrained docking between AGO2 and tubulin-A1A was performed, as previously described (42), using 6WSL.A (43). Interacting residues of tubulin-G1, within the γ-tubulin ring (PDB ID: 6V6S) (44), were excluded from docking between AGO2 and tubulin-G1 (PDB ID: 3CB2.A) (45). Structures 6EJ5.A, 8EBX.J and 3CB2.A were retrieved from Research Collaboratory for Structural Bioinformatics (RCSB) PDB (46), and refined with PDBFixer (version 1.9) (47) and APBS-PDB2PQR (version 3.6.2) (48).

DICER structure (PDB ID: 7XW3.A) (49) from RCSB PDB was processed with EasyModel Server (50) via Basic Modelling/Loop Refining (51) (1,450-1,470 residue range) and APBS-PDB2PQR (48). As DICER is a large protein, docking between AGO2 PIWI and DICER RNAse III A was performed, since these domains are known to interact, as based on experimental evidence (52). Each detection of interfacing residues relied on the PDBSum Server (53), while the dissociation constant (K_d) of the hypothetical complex in each docking model was predicted using the Prodigy Server (54). Selection of docking models and heatmap production for the computed K_d values were generated, as previously described (42). Predictions of whole-structure DICER-AGO2 and CEP250-AGO2 putative complexes were performed by the AlphaFold Server (55), using protein sequences from UniProt (56) (seed=42). Output files were converted to PDB format using Gemmi (version 0.7.0) (57), for compatibility with PDBsum and Prodigy Server. As AlphaFold Server provides five outputs per complex, the predicted DICER-AGO2 complex that features the PIWI domain at the interphase between DICER and AGO2 was selected, as previously described (51). Concerning the CEP250-AGO2 presumable complex, selection of the output was made according to the predicted K_d value by Prodigy Server. A comparative heatmap, including the K_d values of all putative complexes, was generated, using the Seaborn (/joss.theoj.org/papers/10.21105/joss.03021) (version 0.12) Python Package. VMD (version 1.9.3) (58) and ChimeraX (version 1.9) (59) were used for visualizing the docking models and predicted complexes, respectively.

Molecular mapping of AGO2 protein-protein interactions was conducted via the IntAct Molecular Interaction Database (EMBL-EBI; Wellcome Genome Campus) (60).

Results

Cytoplasmic distribution of the AGO2 protein in LX-2 cells, during interphase: Coupling of punctate patterning with local homeostasis. Specificity of the anti-AGO2 antibody used in the present study was verified by transfecting human stellate liver (LX-2) cells with a plasmid (EGFP-hAgo2) responsible for the overexpression of human AGO2 protein fused to the (enhanced) green fluorescent protein (GFP). GFP served as an imaging reporter for its sub-cellular visualization and detection. Following GFP-AGO2 overexpression, LX-2 cells were processed for targeted immuno-localization of the endogenous AGO2 protein (red). GFP-AGO2 overlapped with the red AGO2-signals (Fig. 1), demonstrating that the antibody used in the present study specifically bound human AGO2 protein, in liver cells. Furthermore, GFP did not alter AGO2 ability to be recognized by the, herein, used antibody, thereby indicating that, besides antigenicity, both locality and interactivity of GFP-AGO2 have to remain unaffected, presenting highly similar profiles to the endogenous AGO2-specific ones. The AGO2-specific (overlap; yellow) punctate pattern in the LX-2 cytoplasm suggests key essential roles of the protein in the control of local homeostasis during interphase of human liver cells. An AGO2-dependent operation of the RNAi machinery in multiple cytoplasmic foci/bodies (such as P-bodies) (61) at the interphase stage (Fig. 1) may indicate the locality-dependent regulation of sub-cellular homeostasis at the mRNA stability (or translation) level.

Novel patterns of AGO2 compartmentalization in human liver cells undergoing mitosis: Non-canonical, RNAi-dependent, activity in centrosomes, mitotic spindles and cytokinetic bridges during cell division. Sub-cellular localization profiles of the AGO2 protein in LX-2 cells undergoing mitosis were investigated. Despite its cytoplasmic distribution in the form of punctate bodies at the interphase stage (Figs. 1 and 2), AGO2 protein presented novel localization patterns at the mitotic stages of dividing LX-2 cells. AGO2 was immuno-detected in the centrosomes, mitotic spindle and cytokinetic bridge, also exhibiting similarities to the α-tubulin-dependent cytoskeletal network during mitotic, but not interphase, stages (Figs. 2 and S1A-D), thereby indicating a novel, non-canonical, RNAi-dependent, activity of AGO2 in mitotic apparatus, to likely ensure local homeostasis.

Oncogenic signatures of HepG2 human liver cancer cells do not impair AGO2-topology profiling during mitosis. To examine the role of oncogenicity in AGO2-specific patterning during the cell cycle, AGO2 sub-cellular distribution in HepG2 human

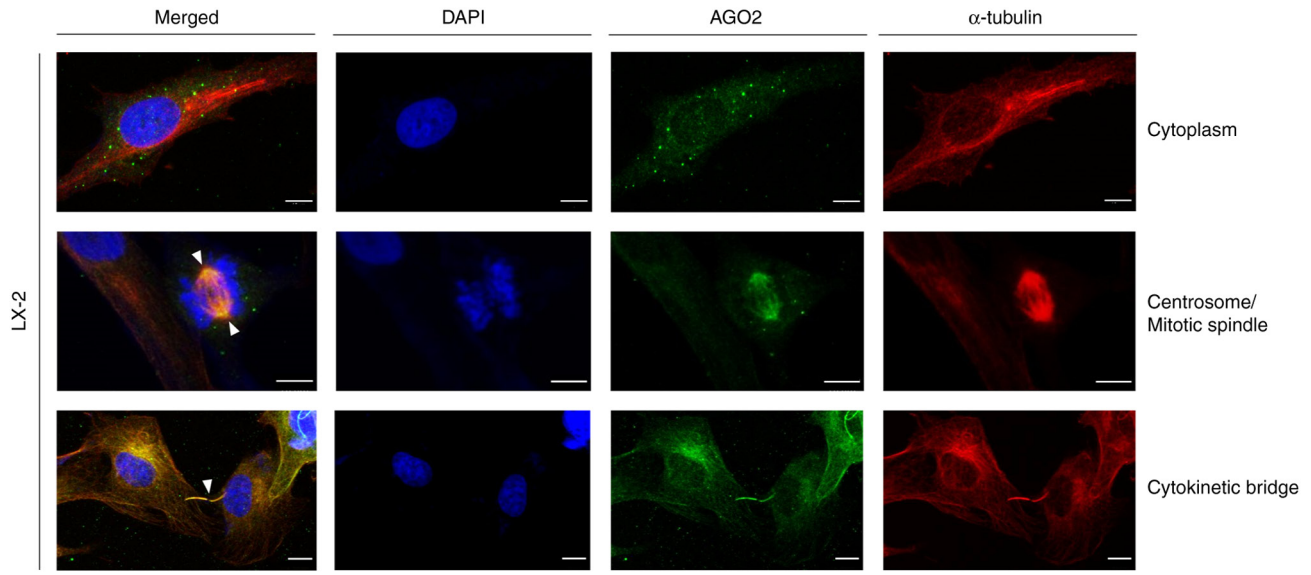

Figure 2. AGO2 distribution profiling in LX-2 liver cells undergoing mitosis. Confocal laser scanning microscopy of LX-2 cells during interphase and mitosis demonstrating endogenous AGO2 protein expression and distribution in the cytoplasm of interphase cells (punctuate pattern), and in the centrosome, mitotic spindle and cytokinetic bridge of mitotic cells (white arrowheads). Nuclear/chromosomal DNA is indicated in blue by DAPI. Yellow is produced by the overlap of green and red. Scale bar, 10 μm. AGO2, argonaute RNA-induced silencing complex catalytic component 2.

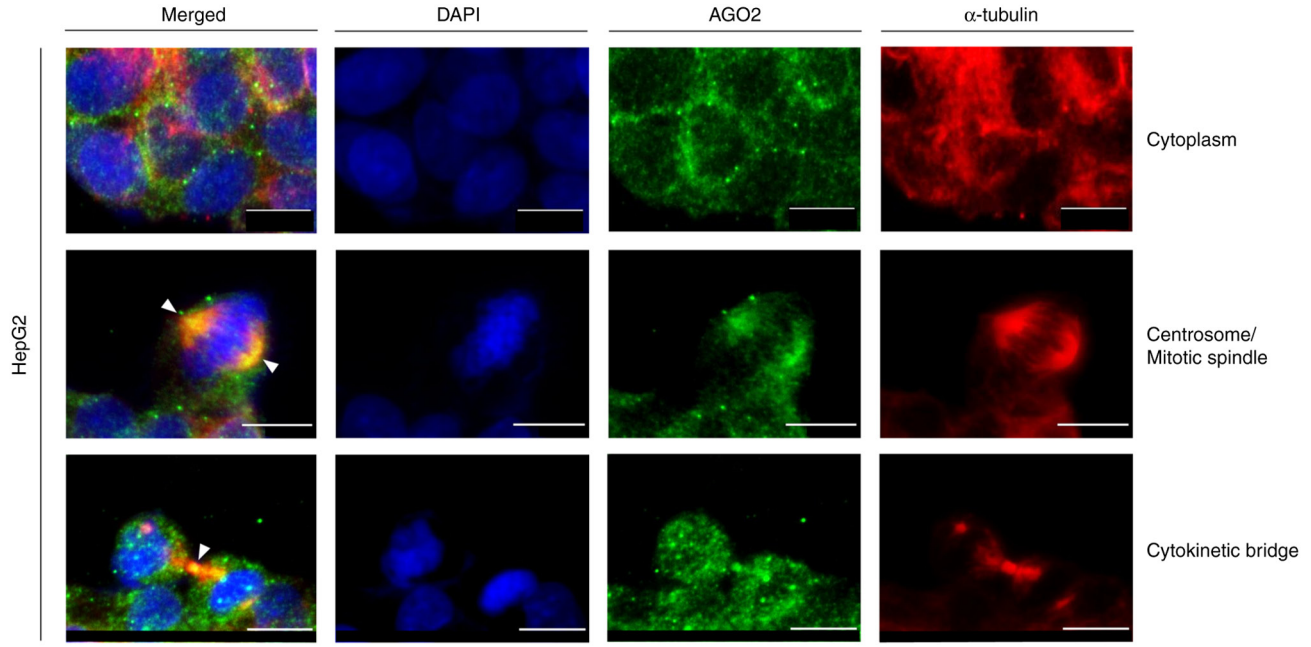

Figure 3. Localization of AGO2 protein in HepG2 liver cancer cells during mitosis. Confocal laser scanning microscopy immunofluorescence images of HepG2 cells at the interphase and mitotic stages, demonstrating AGO2 protein expression and distribution in the cytoplasm at interphase, and in the centrosome, mitotic spindle and cytokinetic bridge (white arrowheads) during mitosis of dividing cells. Nuclear/chromosomal DNA is indicated in blue by DAPI. Yellow, merger of green and red. Scale bar, 10 μm. AGO2, argonaute RNA-induced silencing complex catalytic component 2.

liver cancer cells undergoing mitosis was immuno-profiled. Similarly to LX-2, HepG2 dividing cells were characterized by AGO2-localization patterns in the centrosomes, mitotic spindle and cytokinetic bridges of mitotic cells (Fig. 3). A cytoplasmic, punctate pattern of AGO2 topology was observed in HepG2 cells during interphase, demonstrating compartmentalization similar to LX-2 cells, both at the interphase and mitosis stages. Liver oncogenicity did not alter AGO2 patterning during cell division, thereby indicating the malignancy-independent role of AGO2 protein in controlling local homeostasis via canonical, RNAi-dependent (at interphase), or non-canonical, RNAi-dependent (at mitosis), mechanisms.

Co-localization of AGO2 with key centrosomal proteins reveals a potential role in the centrosome of LX-2 dividing cells. Given the novel immuno-detection profiling of AGO2 protein in liver centrosomes, its co-localization landscape was mapped with key centrosomal (centriolar or PCM) proteins.

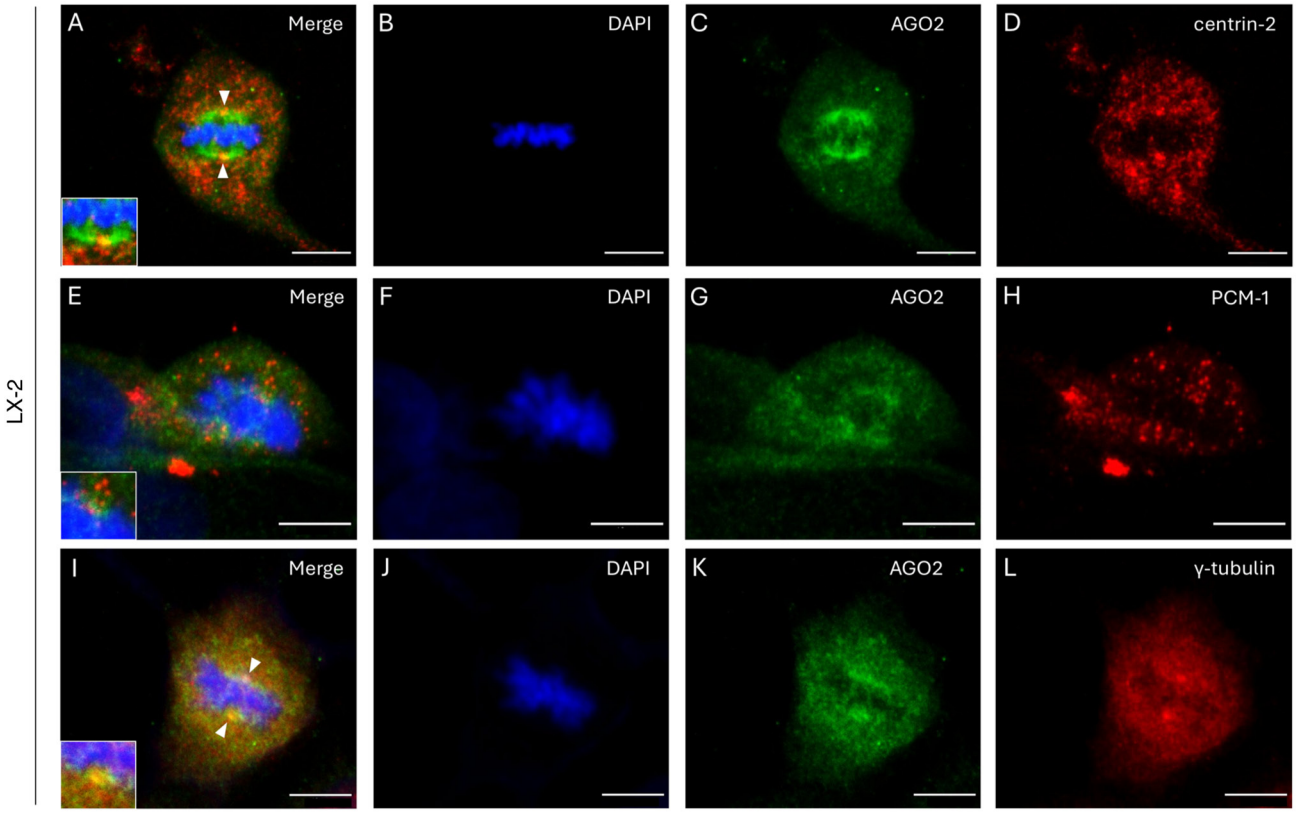

Figure 4. Co-localization of AGO2 with centrin-2 and γ-tubulin centrosomal proteins during cell cycle. Confocal laser scanning microscopy immunofluorescence images of LX-2 liver cells, showing co-localization patterns (white arrowheads) of AGO2 protein with key (A-D) centrosomal components centrin-2 (centriolar protein) and (I-L) γ-tubulin (PCM protein). (E-H) PCM-1 did not co-localize with AGO2. Cell nucleus (chromosomal DNA) is presented in blue by DAPI. Yellow, merge of green and red. Scale bar, 10 μm. AGO2, argonaute RNA-induced silencing complex catalytic component 2; PCM-1, peri-centriolar-material 1.

Immunofluorescence imaging of LX-2 mitotic cells revealed co-localization pattern of AGO2 with centrin-2 (Fig. 4A-D), a key structural component of centrioles (62-64). Notably, AGO2 was also co-localized with γ-tubulin, a protein that serves as a template for the initiation of α- and β-tubulin heterodimer polymerization at the PCM area (64-66), in several of the examined cells (Fig. 4I-L). PCM-1 protein, a component of centriolar satellites/PCM mass (64,67,68), was not observed in proximity to AGO2 (Fig. 4E-H), indicating a novel, non-canonical, RNAi-dependent, role for the AGO2 protein in γ-tubulin-linked, but not PCM-1-associated, peri-centriolar material, in liver cells. Of note, the PCM area comprised distinct structural 'niches' (or layers) with different protein compositions among them; for example, one niche contained γ-tubulin and AGO2 in proximity to each other (γ-tubulin/AGO2 co-localization) (Fig. 4I-L), whereas another contained PCM-1 in the absence of AGO2 (lack of PCM-1/AGO2 co-localization; Fig. 4E-H).

AGO2-localization patterning in LX-2 cell cycle stages. To determine AGO2-specific localization profiles throughout cell division, the sub-cellular topology of AGO2 was observed at each stage of mitosis and interphase in LX-2 dividing cells. AGO2 was immuno-detected in LX-2 centrosomes at the interphase and early prophase stages, while AGO2 distribution was similar to α-tubulin patterning during mitotic spindle formation at the metaphase stage, without alteration until late anaphase (Figs. 5 and S1A). During the subsequent cell cycle stages of telophase and cytokinesis, AGO2 was observed in the cytokinetic bridge between the daughter cells (Fig. 5). AGO2 was localized in an interior area of the cytokinetic bridge, forming fibrillar-like structures (Figs. 5 and S1C), which may stabilize the integrity of the bridge in a non-canonical, RNAi-dependent, manner. Taken together, the present data suggest novel sub-cellular topologies of AGO2, which may be associated with its role in the efficient operation of cell division machinery.

Centrosomal co-localization of AGO2 and DICER proteins in LX-2 cells undergoing mitosis: Non-canonical, RNAi-dependent, control of local homeostasis. Since AGO2 forms the protein core of the RISC complex, it was hypothesized that other RISC components may also reside in key mitotic structures of dividing cells. Hence, the overlapping topology and distribution patterns of AGO2, DICER and TRBP2 proteins in LX-2 cells were examined. At the interphase stage, AGO2 co-localized with DICER in several cytoplasmic foci/bodies (potentially P-bodies; Fig. 6), directly reflecting their locality-dependent joint action in the RNAi mechanism. During mitosis, a co-localization pattern of AGO2 and DICER proteins was detected in liver centrosomes (Figs. 6 and S1E), whereas at the cytokinesis stage, AGO2 and DICER presented distinct sub-cellular compartmentalization profiles; AGO2 resided in the cytokinetic bridge, while DICER was located in the midbody structure (Figs. 6 and S1F). Despite their different distribution, overlap suggested the locality-dependent functionality of RNAi machinery at the cytokinetic bridge/midbody 'borders'.

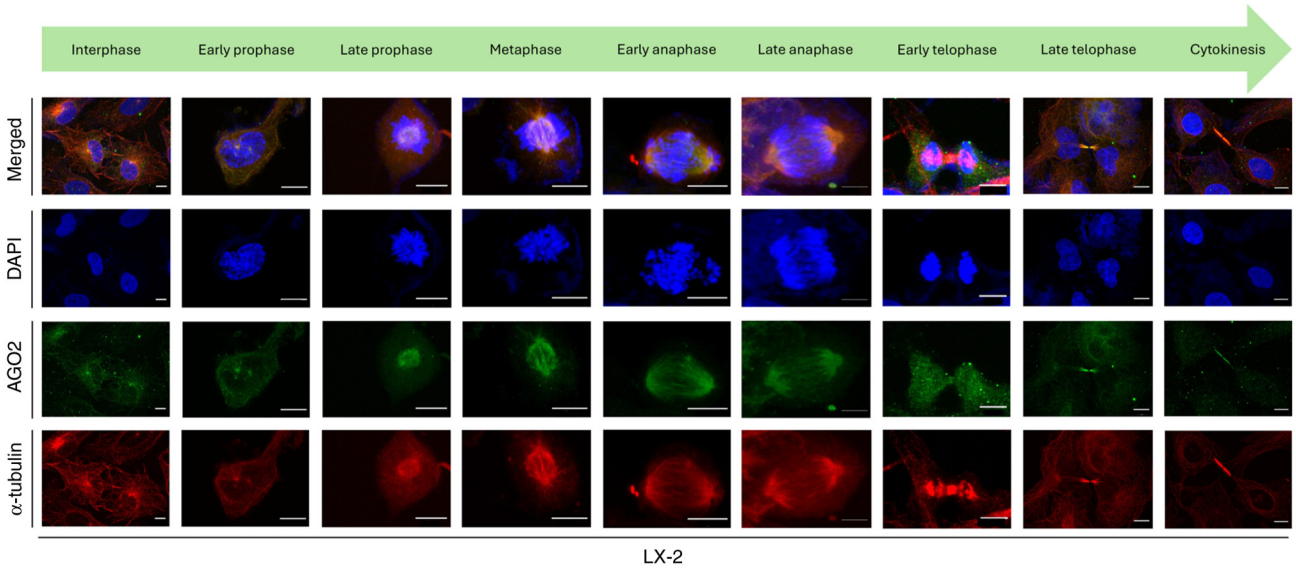

Figure 5. AGO2 protein distribution in LX-2 cells undergoing mitosis. Confocal laser scanning microscopy immunofluorescence images of LX-2 hepatic/liver cells, presenting AGO2 localization patterns at different stages of mitosis. Nuclear/chromosomal DNA is presented in blue by DAPI. Yellow, merger of green and red. Scale bar, 10 μm. AGO2, argonaute RNA-induced silencing complex catalytic component 2.

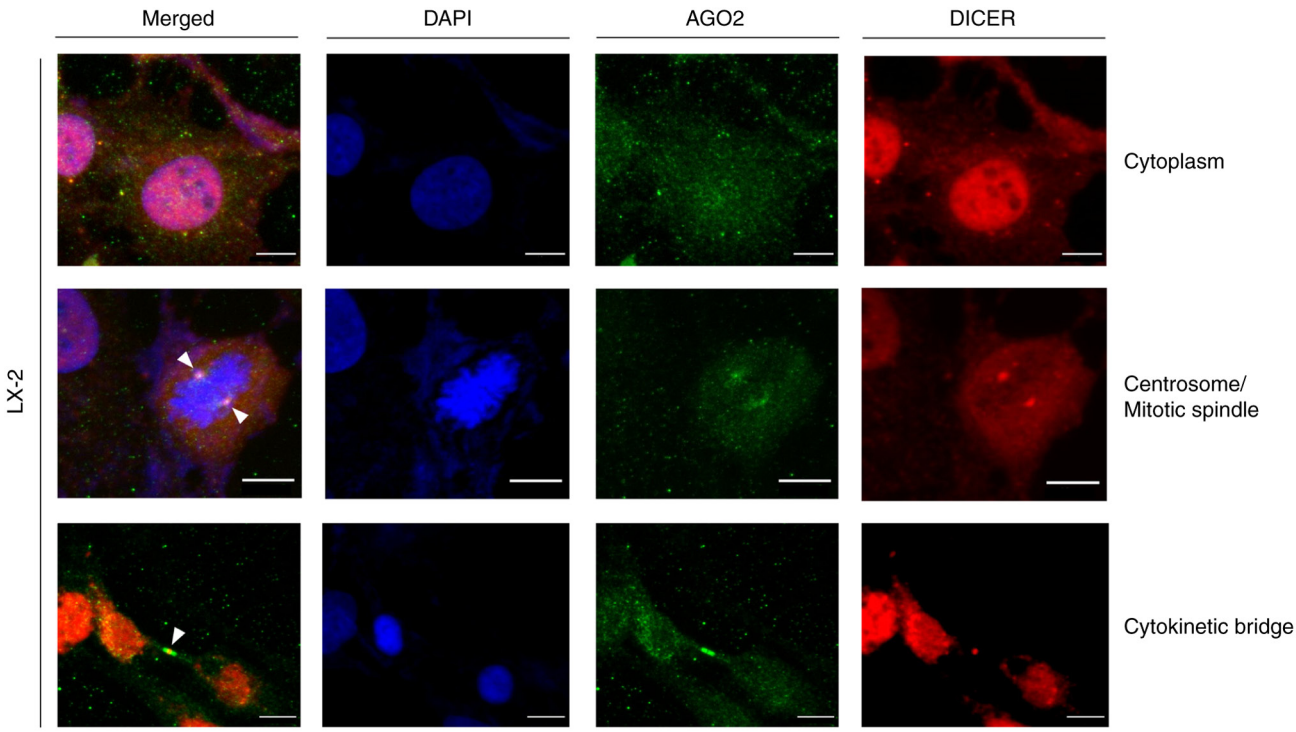

Figure 6. Co-localization of AGO2 and DICER proteins in LX-2 liver cells undergoing mitosis. Immunofluorescence confocal laser scanning microscopy of centrosome- and cytokinetic bridge-specific co-localization of the AGO2 and DICER proteins in LX-2 mitotic cells (white arrowheads). Nuclear/chromosomal DNA is shown in blue by DAPI. Yellow, merger of green and red. Scale bar, 10 μm. AGO2, argonaute RNA-induced silencing complex catalytic component 2; DICER, double-stranded RNA endoribonuclease.

The TRBP2 protein, a key component of the RNAi machinery that undergoes cell cycle regulation (42), was not co-localized with AGO2 at any mitotic apparatus (Fig. 7), suggesting the non-canonical, RNAi-dependent, role of AGO2 and DICER joint actions in the LX-2 centrosome and cytokinetic bridge. AGO2 and DICER may function together, in the absence of TRBP2, in a non-canonical, RNAi-dependent, manner, to control local homeostasis at the centrosomal and cytokinetic bridge level in liver cells.

AGO2 does not require UPF1 activity in the centrosome/mitotic spindle/cytokinetic bridge mitotic pathway of LX-2 dividing cells. To investigate RNA binding proteins (RBPs) other than AGO2 and their capacity to compartmentalize

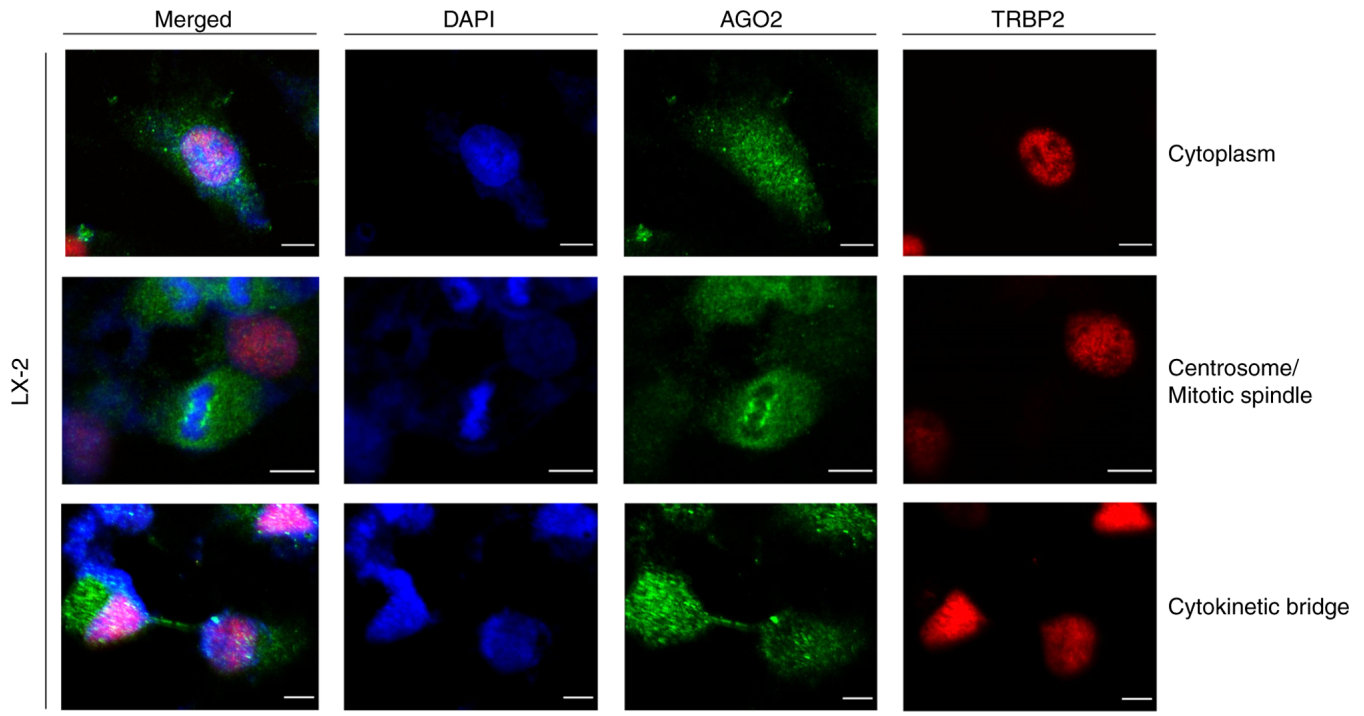

Figure 7. TRBP2 does not co-compartmentalize with AGO2 in LX-2 hepatic/liver cells. Confocal laser scanning microscopy immunofluorescence images of LX-2 dividing cells demonstrating the absence of AGO2 and TRBP2 co-localization in the centrosome, mitotic spindle and cytokinetic bridge apparatuses during mitosis. There was no TRBP2 detection at the anaphase stage in LX-2 mitotic cells (middle panels). Nuclear/chromosomal DNA is presented in blue by DAPI. Scale bar, 10 μm. AGO2, argonaute RNA-induced silencing complex catalytic component 2; TRBP2, transactivation response element RNA-binding protein.

in the centrosome, mitotic spindle and/or cytokinetic bridge mitotic machinery, UPF1, a key RBP family member and AGO2 interactor (69), was next examined. UPF1 is a monomeric RNA helicase that co-localizes with AGO2 in processing bodies (potentially P-bodies) and contributes to the RNA silencing program (70-72). Hence, localization of both proteins was imaged in control and LX-2 cells transfected with the EGFP-hAgo2 and RNT1-GFP plasmids, responsible for the overexpression of GFP-AGO2 and GFP-UPF1 chimeric proteins, respectively. In control [transiently transfected with the empty vector pcDNA3.1(+)] cells, the endogenous AGO2 and UPF1 proteins presented weak co-localization in the cytoplasm, but not in the nucleus, of LX-2 interphase cells (Fig. 8A). Similarly, the overexpression of AGO2 (GFP-AGO2) protein did not cause notable co-localization with endogenous UPF1, whereas the UPF1 (GFP-UPF1) overexpression resulted in a strong, punctate co-localization profile with endogenous AGO2, with the two proteins being immuno-detected in the same sub-population of cytoplasmic foci/bodies of LX-2 interphase cells (Fig. 8B and C). To ensure technical integrity, target specificity of the anti-UPF1 antibody was checked by transiently transfecting LX-2 cells with the RNT1-GFP expression plasmid, and transfected cells were stained with the anti-UPF1 antibody to obtain overlapping (yellow) signals (Fig. S2). To confirm reliability of the data, the distribution of both AGO2 and UPF1 proteins were separately examined in LX-2 cells, transiently transfected with the empty vector pcDNA3.1(+) (Fig. S3).

The present data suggest GFP did not disturb UPF1 capacity to be specifically recognized by the antibody, likely indicating unimpaired antigenicity that is mechanistically coupled with undisturbed locality and interactivity, in the GFP-UPF1 molecular context and LX-2 cytoplasm setting. UPF1 (GFP-UPF1) overexpression induced cytoplasmic accumulation of UPF1-containing foci/bodies, with a distinct sub-population carrying both UPF1 (GFP-UPF1) and AGO2 (endogenous) proteins (yellow), suggesting their cooperative actions in the RNA silencing process. Concentration-dependent formation of UPF1-bodies may induce AGO2 recruitment to generate UPF1/AGO2-bodies in a locality-specific manner.

To determine the UPF1 sub-cellular patterning towards mitosis, endogenous UPF1 immuno-detection profiles were obtained from LX-2 dividing cells. UPF1 and α-tubulin (a structural component of microtubule networks) distribution profiles were not similar to each other, either in interphase or in mitotic LX-2 cells, since the UPF1 protein was missing from the centrosome/mitotic spindle/cytokinetic bridge pathway that mechanistically typifies mitosis (Fig. 9). Taken together, the present data demonstrated the capacity of AGO2, but not other RBPs, such as UPF1, to specifically control structural architecture and/or functional integrity of the centrosome, mitotic spindle and cytokinetic bridge assemblies, in a non-canonical, RNAi-dependent mode to provide spatial and temporal homeostasis.

Microtubule-network disruption impairs AGO2 distribution patterns in LX-2 cells. AGO2 and α-tubulin exhibited similar sub-cellular distribution patterns, especially during centrosome/mitotic spindle and cytokinetic bridge formation,

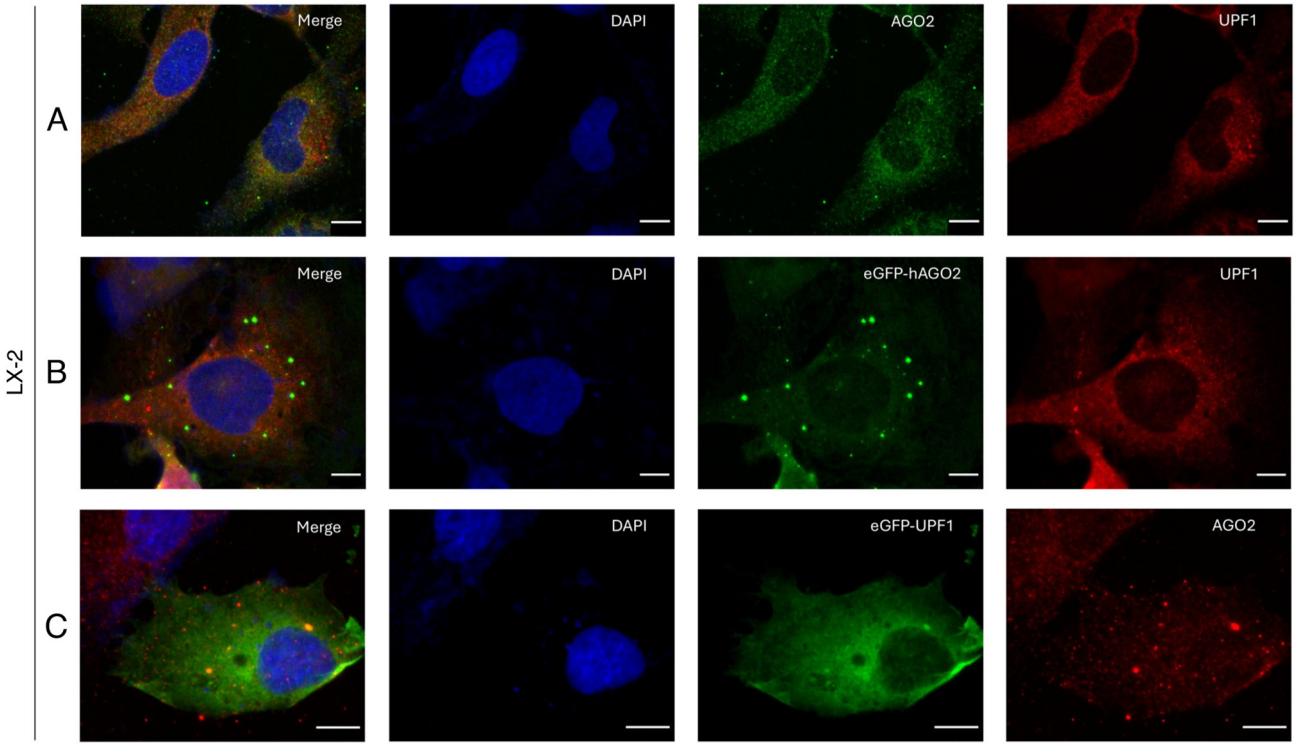

Figure 8. AGO2 and UPF1 distribution in LX-2 interphase cells. Confocal laser scanning microscopy immunofluorescence images of LX-2 hepatic/liver cells at the interphase stage, showing cytoplasmic localization patterns of endogenous (A) AGO2 and UPF1 protein expression in control, (B) UPF1 and eGFP-hAGO2 protein expression in the AGO2-overexpressing cells and (C) AGO2 and eGFP-UPF1 protein expression in UPF1-overexpressing cells. Nuclear/chromosomal DNA is presented in blue by DAPI. Yellow (punctate cytoplasmic patterning), merge of green and red. Scale bar, 10 μm. AGO2, argonaute RNA-induced silencing complex catalytic component 2; UPF1, up-frameshift protein 1.

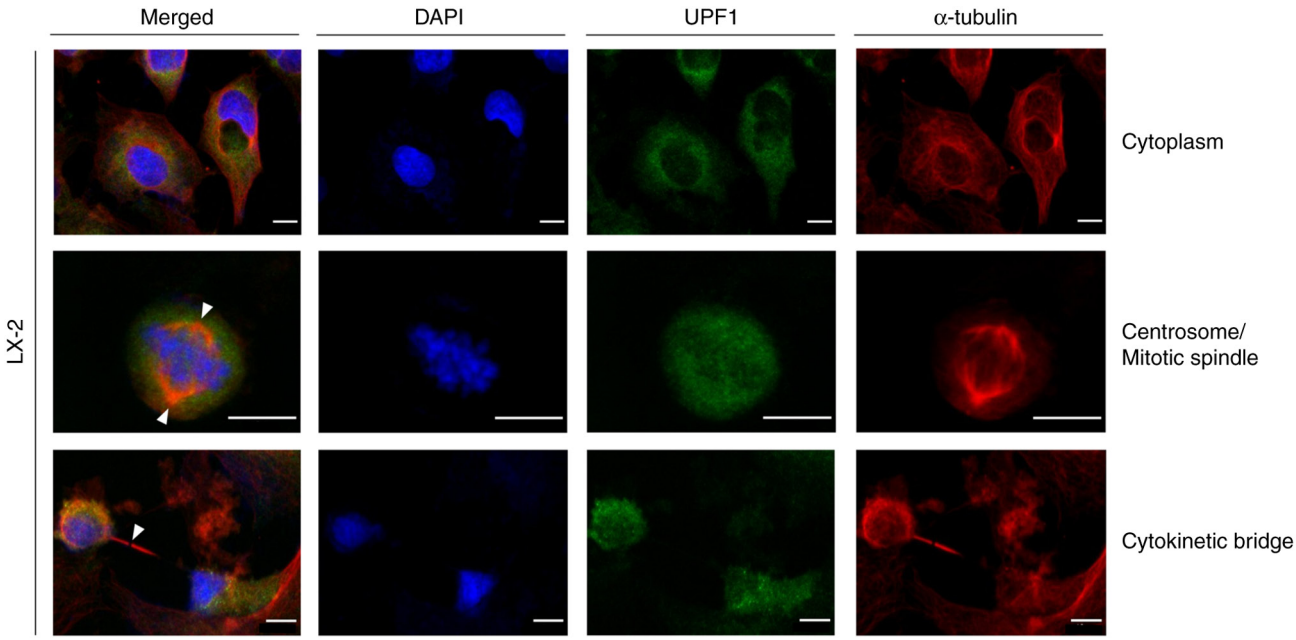

Figure 9. UPF1 does not compartmentalize with α-tubulin in mitotic apparatuses during LX-2 cell division. Confocal laser scanning microscopy immunofluorescence images of centrosome, mitotic spindle and cytokinetic bridge machineries (containing α-tubulin as a major structural component) (white arrowheads) lacking UPF1 localization in LX-2 hepatic/liver cells undergoing mitosis. Nuclear/chromatin DNA is shown in blue by DAPI. Scale bar, 10 μm. UPF1, up-frameshift protein 1.

leading to the hypothesis that the two proteins may physically interact and exhibit crosstalk in a locality-dependent manner. A clinically relevant concentration of demecolcine (0.4 μg/μl), a potent microtubule-polymerization inhibitor, was administered to LX-2 cells, to disintegrate the cytoskeletal system. A complete disruption of the microtubule network was observed

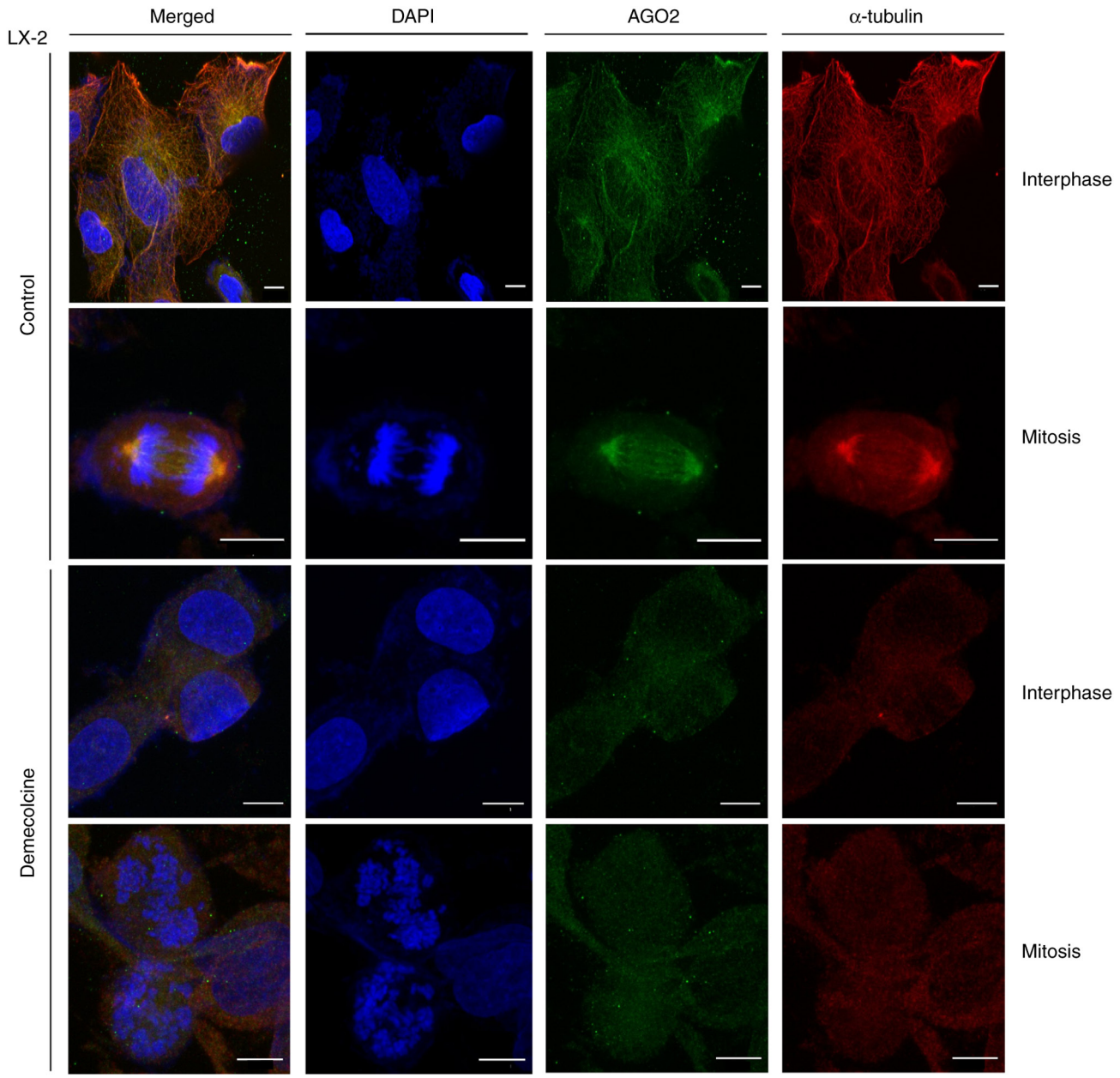

Figure 10. Microtubule network disintegration causes disruption of AGO2 mitotic patterning in LX-2 dividing cells. Confocal laser scanning microscopy immunofluorescence images of LX-2 hepatic/liver cells, presenting AGO2 distribution, in control (DMSO) and microtubule polymerization inhibitor demecolcine-treated (0.4 μg/μl; 6 h) mitotic and interphase cells. In response to demecolcine, AGO2 protein loses its centrosome/mitotic spindle axis localization pattern at mitosis and its cytoplasmic compartmentalization at interphase. Nuclear/chromatin DNA is indicated in blue by DAPI. Scale bar, 10 μm. AGO2, argonaute RNA-induced silencing complex catalytic component 2.

6 h post-administration, with AGO2 also losing its typical, canonical, immuno-localization pattern in LX-2 interphase cells (Fig. 10). During cell division, both centrosome and mitotic spindle were lost, and the AGO2-specific foci in the centrosome/mitotic spindle axis were also absent (Figs. 10 and S1D), demonstrating the ability of fibrillar α-tubulin to regulate the recruitment of AGO2 protein in the centrosome and mitotic spindle assembly of diving cells, to maintain spatial and temporal homeostasis in liver-cell normal settings.

AGO2 localization in mitotic apparatus was observed in cases of abnormal cell divisions. In rare LX-2 cell sub-populations characterized by aberrant number, geometry and topology of centrosomes and mitotic spindles (such as multi-polar spindles), AGO2 co-localized with α-tubulin in all pathogenic/pre-oncogenic assemblies (Fig. 11), demonstrating the importance of AGO2 protein in centrosome/mitotic spindle biosynthesis and structural/functional integrity in dividing liver cells undergoing mitotic stress. Removal or elimination of AGO2 protein, specifically from multi-polar spindles, may inhibit the transition from a pre-oncogenic to an oncogenic cell state, thereby opening a novel therapeutic window of locality-dependent AGO2 activity suppression against human malignancies, including liver cancer. To determine the involvement of AGO2 in tumorigenesis, the interactome landscape of AGO2 protein has been mapped (60). AGO2 is characterized by a plethora of interactions, with several of its interactors being affected by driver oncogenic mutations in human cells (Fig. S4).

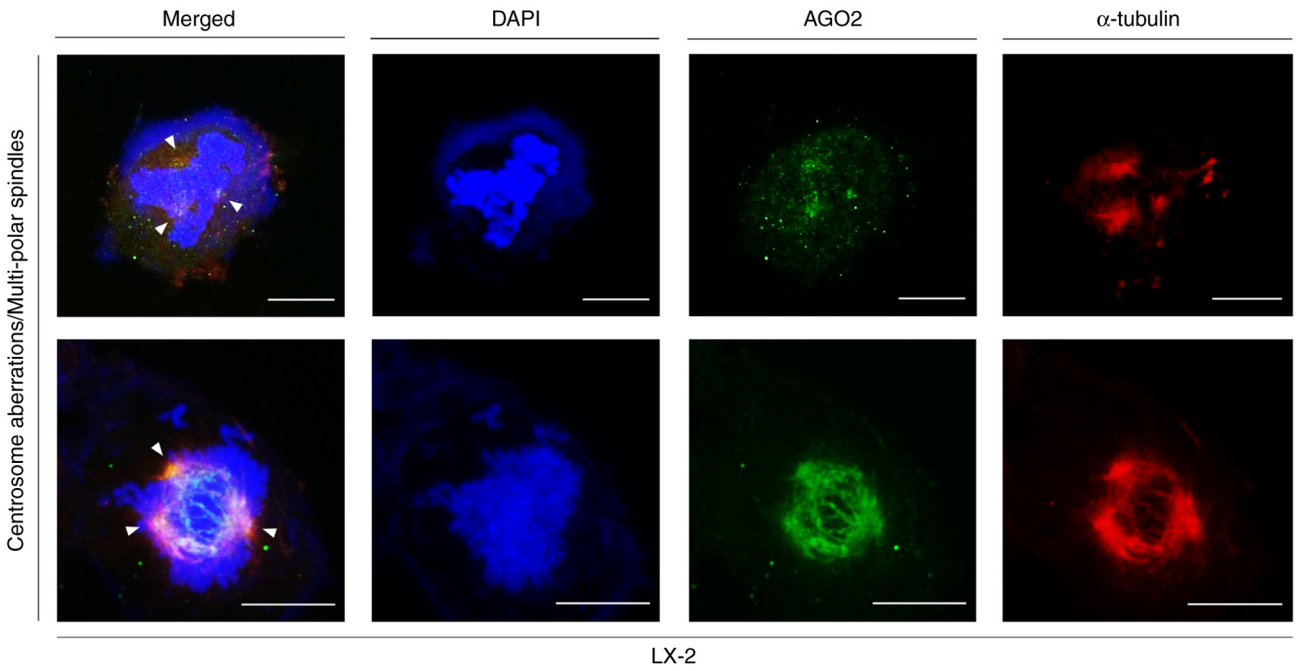

Figure 11. Centrosome/mitotic spindle aberrations do not alter mitotic co-localization of AGO2 and α-tubulin proteins in LX-2 dividing cells. Confocal laser scanning microscopy immunofluorescence images of rare LX-2 liver cell sub-populations carrying aberrant (number, geometry, topology and architecture) centrosome and mitotic spindle structures (multi-polar spindles). AGO2 and α-tubulin co-localization patterning was observed in aberrant mitotic apparatuses (white arrowheads). Nuclear/chromatin DNA is indicated in blue by DAPI. Yellow, merge of green and red. Scale bar, 10 μm. AGO2, argonaute RNA-induced silencing complex catalytic component 2.

Molecular modelling of AGO2 protein-protein interactions. AGO2 protein-protein interaction profiling was examined, through an advanced *in silico* molecular modelling approach. Docking tests were carried out between AGO2 and its (known or potential) interactors, including α- and γ-tubulin, centrin-2, DICER and UPF1 proteins. *In silico*, AGO2 was able to recognize and bind proteins that immuno-co-localized with AGO2 in liver cells (Figs. 12A and S5). DICER (first) and centrin-2 (second) displayed the highest AGO2-binding activity, according to their comparatively low K_d values, which denoted intrinsic structural stability of protein-containing bi-molecular complexes (Fig. 12B). These molecular modelling metrics corroborate the immunofluorescence-derived co-localization patterns, indicating joint actions between partners (for example, AGO2, centrin-2 and DICER), to control local (for example, centrosomal) homeostasis, during mitosis. α-tubulin had the lowest AGO2-binding capacity (highest K_d) among proteins (Fig. 12B), thus indicating the contribution of additional co-factors to strengthen the interaction. Furthermore, AGO2 is as an interactome component (interactor) of CEP250 (centrosomal protein 250), a centriole linker protein with disordered regions that, due to high plasticity levels, promote multivalent interactions at the centrosome (73). Molecular modelling tests assess the CEP250-AGO2 complex stability *in silico* (Fig. S6), indicating a novel role of AGO2 in controlling CEP250-specific, local, homeostasis at the centriole linker sub-compartment.

Discussion

AGO2 protein forms the core of the RISC complex and serves an essential function in miRNA-dependent gene expression regulation via the canonical RNAi mechanism. AGO2 serves key roles in biological processes, including embryonic development, cell differentiation, anti-viral defence and transposon silencing (25,74-77). Furthermore, a number of reports have revealed the role of AGO2 in pathological conditions, such as abnormal neurological development, infertility and tumorigenesis (75,78,79). Notably, AGO2 is present in sub-cellular areas, such as the GW (glycine/tryptophan)- and P (processing)-bodies, stress granules, along apical junctions and *Drosophila* nanotubes, while an association with endosomes at synapses has also been reported (80-84). Notably, our previous study demonstrated AGO2 localization in tubular protrusions of human thyroid cells (17).

The present findings revealed AGO2 localization in centrosomes and mitotic spindles, and demonstrate AGO2 presence in cytokinetic bridges of both normal liver and liver cancer cell lines (LX-2 and HepG2, respectively). To the best of our knowledge, the present study is the first to describe the molecular composition of an alternative, non-canonical RNAi machinery that contains AGO2 and DICER, but lacks TRBP2 and UPF1, and functions in specific intracellular contexts, such as the centrosome, mitotic spindle and cytokinetic bridge apparatuses, during the cell cycle of human liver cells. In addition to the oncogenic (HepG2) and non-oncogenic (LX-2) liver cells in the present study, normal human primary thyroid follicular epithelial cells (NTHY-ori 3-1) accommodate AGO2 in tunnelling nanotubes and cytokinetic bridges (17), indicating the universality of RNAi machinery variations associated with AGO2 functional nuances. Nevertheless, additional cell types of diverse tissue origin, oncogenic state and mutational signature, should be

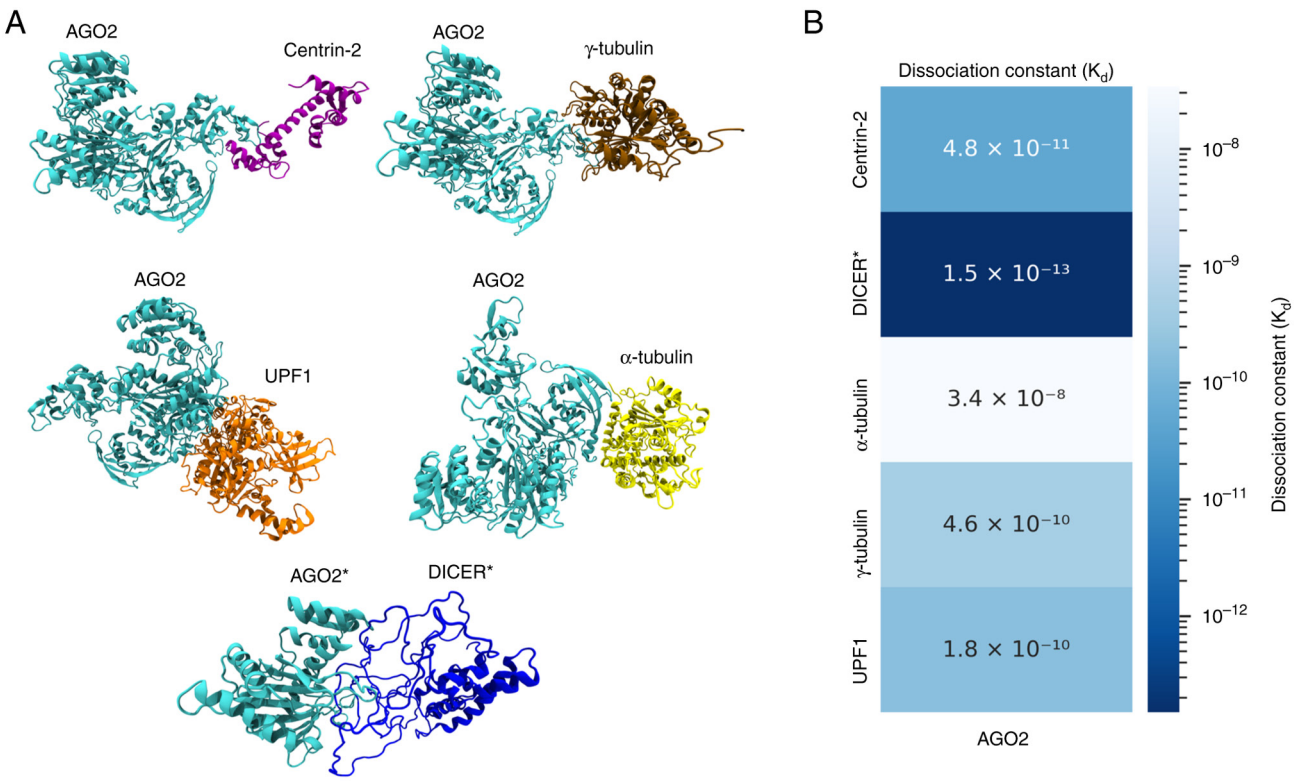

Figure 12. Molecular modelling of AGO2 protein-AGO2 protein-interactor complexes. Docking tests between AGO2 and potential interacting proteins. (A) Predicted 3D molecular models of AGO2 protein with interactors, such as centrin-2, γ-tubulin, UPF1, α-tubulin and DICER* proteins. (B) Dissociation constant (K_d) values, indicating the possibility (complex stability) of bi-molecular binding between AGO2 and putative interactors centrin-2, γ-tubulin, UPF1, α-tubulin and DICER*. *Constrained docking between the AGO2 PIWI (position: 517-818th aa; 301 residues) and the DICER RNase III A domain (position: 1,295-1,596th aa; 301 residues). AGO2, argonaute RNA-induced silencing complex catalytic component 2; aa, amino acid; DICER, double-stranded RNA endoribonuclease; UPF1, up-frameshift protein 1.

assessed to demonstrate the general and universal characteristics of the AGO2 locality profiles and their non-canonical, RNAi-mediated, regulatory networks.

AGO2 exerts oncogenic activities, since it is involved in cellular transformation and tumorigenesis in numerous types of cancer, including liver, hypopharyngeal, colon, ovarian and gastric cancer, promoting cell proliferation, metastasis and angiogenesis (85-92). However, in certain cases, such as lung and breast cancer and melanoma, AGO2 serves as a tumour suppressor, decreasing proliferation and motility of cancer cells (75,93,94). Regardless of its tumor-promoting or -suppressing activities, AGO2 has emerged as a key regulator of oncogenesis, potentially exerting cellular context-dependent effects in versatile and multifaceted manners (12). AGO2 interactome maps contain key bi-molecular interactions between AGO2 and the EGFR (epidermal growth factor receptor), LIMD1 (LIM domain containing 1) and MTDH (Metadherin) proteins, which control key oncogenic pathways, thus indicating the clinical applicability of AGO2-based therapeutic strategies.

AGO2 homozygous null (*AGO2*$^{-/-}$) mice display embryonic lethality characterized by neural-tube defects, abnormal forebrain patterning, enlarged hearts, pericardial swelling, delayed development, and defects in yolk sac and placenta (95-97). *In vivo* studies (for example, *AGO2*$^{+/+}$ vs. *AGO2*$^{-/-}$ mice) of centrosome-, mitotic spindle- and cytokinetic bridge-specific structural integrity and functional capacity cannot be mechanistically performed in diverse organs, tissue and cell populations derived from adult *AGO2*$^{-/-}$ mice. Therefore, novel tools and advanced technology are required to distinguish RNAi-dependent from -independent, AGO2-containing protein networks, *in vivo*. Experimental validation of the proposed 'AGO2-centric' therapeutic platform in next-generation animal models may facilitate novel drug schemes offering strong chemotherapeutic benefits in patients with aggressive malignancies.

The localization of AGO2 protein in the centrosome and its potential interaction with centrosomal proteins (indicated by immuno-detection and molecular docking assay, respectively), together with AGO2 centrosomal topology at all stages of mitosis, demonstrated new roles for AGO2 in centrosome pathophysiology. In accordance, GW/P-body populations, marked by GW182 and hAGO2 proteins, reside in the centrosome of numerous types of cell during interphase (98,99). Molecular modelling of CEP250-AGO2 complex indicates a novel role of AGO2 in regulating CEP250-dependent, local, homeostasis at the centriole linker structure. Moreover, centriole body may also recruit AGO2 in a centrin-2-dependent manner, with AGO2 protein potentially exerting distinct effects in the centriole linker vs. body, ensuring spatiotemporal-specific regulation of homeostasis, during cell division. AGO2 may control linker-mediated cohesion and positioning of centrioles/centrosomes, and body-derived integrity and stability of centrioles/centrosomes at all mitosis stages. Since a number of specific RNA species reside at the centrosome (100-104), AGO2 may serve as a 'molecular barrier' against the harmful

accumulation of non-specific RNA transcripts, which may be eliminated via a centrosome-specific AGO2/RNAi machinery.

The centrosome-specific co-localization of AGO2 and DICER proteins underpins their essential roles as fundamental components of the RNAi mechanism that controls local homeostasis during cell cycle progression. However, the inability of TRBP2 to co-localize with AGO2 indicates a novel, TRBP2-independent, RNAi machinery, which uses an AGO2-DICER-containing complex that lacks TRBP2, to safeguard centrosomal RNAs from contamination with cytoplasmic transcripts, exhibiting either non-essential activity or synthesizing toxic products against centrosome functions, during mitosis. The novel, AGO2-DICER-dependent and TRBP2-independent apparatus may target and eliminate RNA transcripts leaked from the cytoplasm to the centrosome. Centrosomes and cytokinetic bridges may recruit non-canonical ($AGO2^{+}$/$DICER^{+}$/$TRBP2^{-}$) RNAi machinery to locally control RNA homeostasis, by protecting centrosome- and cytokinetic bridge-specific RNAs from cytoplasm-derived RNA species. Upon arrival at the centrosome or the cytokinetic bridge structure, the misdirected cytoplasmic RNAs are subjected to an $AGO2^{+}$/$DICER^{+}$/$TRBP2^{-}$-mediated degradation or translational suppression, via a novel, non-canonical, RNAi machinery, during cell division. It was hypothesized that centrosomes, cytokinetic bridges and mitotic spindles accommodate non-canonical RNAi machinery, to maintain local RNA homeostasis at mitosis.

Nevertheless, the non-canonical RNAi machinery, which may function in a mitotic apparatus-specific manner, needs direct experimental evidence. Single-molecule fluorescence in real-time imaging, spatial (centrosomal) mRNA/small interfering (si)RNA-transcriptomics and RNA-cleavage reaction assays *in vitro* may provide support for the operation of RNAi machinery with non-canonical functionality, specifically at mitotic centrosomes of dividing cells. The present study lacked experimental validation, which is required to develop AGO2-centric therapies in the clinical management of human pathologies, including liver cancer.

As TRBP2 ensures efficient processing of pre-miRNA species in RNA-overpopulated cellular environments (105), the absence of TRBP2 from mitotic centrosomes may be mechanistically associated with the comparatively lower number of RNA molecules residing in these organelles. TRBP2 undergoes mitosis-specific downregulation in several human cancer cell lines of diverse tissue origin (42), supporting a mitotic centrosome-specific non-canonical RNAi mechanism that operates in RNA-underpopulated environments lacking TRBP2 activity.

Nevertheless, an RNAi-independent role of AGO2 in centrosome/mitotic spindle/cytokinetic bridge cannot be excluded. For example, an AGO2-orchestrated recruitment of specific RNA transcripts to mitotic centrosomes may enhance centrosome cohesion by strengthening centriole/centrosome-linker integrity. As AGO2 binds nucleus-specific mRNA (106), nuclear rRNA (107) and nascent tRNA (108,109) species, AGO2 may direct the targeted transport of specific RNAs to the centrosome, with the mobilized transcripts serving as structural components of the centriole/centrosome linker, during the cell cycle. AGO-mRNA associations occur independently of miRNA species, with mRNA-residing guanine-rich motifs controlling the bi-molecular interactions (109,110). Notably, the successful molecular docking of CEP250, a key centriole/centrosome-linker protein (111), with AGO2 supports the role of AGO2 protein in centriole/centrosome linker stability and dynamics in dividing cells undergoing mitosis. Nevertheless, isolating, profiling and characterizing centrosome-specific RNA transcripts transported to the mitotic apparatus in an AGO2-dependent manner is challenging. Although diverse AGO2-RNA interactions can be identified, their mitotic centrosome landscapes cannot be readily and reliably mapped. It is difficult to distinguish between RNA populations that, despite residing in mitotic centrosomes, may derive from an AGO2-dependent mechanism, whereas some may originate from an AGO2-independent mechanism, both controlling RNA-targeted recruitment to the organelle by engagement of different molecular routes.

Molecular modelling of AGO2-containing (bi-) proteinaceous complexes revealed that centrin-2 was the strongest interactor, following DICER. Centrin-2 may serve as a key recruiter of AGO2 to mitotic centrosomes, with the centrin-2-AGO2 complex potentially regulating biogenesis, stability, functionality and homeostasis of centrosome, in both spatial (reflected by co-localization immuno-profiles) and temporal (depending on cell cycle phases) manners. The computational predictions of AGO2-centered interactions should be verified by quantitative approaches, such as fluorescence resonance energy transfer, and immunoprecipitation (IP) and western blotting, to support their biological accuracy and significance. None of the tested AGO2-specific antibodies demonstrated IP reactions, potentially due to epitope masking, or epitope obliteration effects produced by AGO2 participation in (super-)complex mitotic apparatuses (such as centrosomes), which may require AGO2 to either hide or lose its key epitope(s) recognized by primary antibodies for IP assays.

Dividing human liver cells may use non-canonical, RNAi-dependent, machinery that contains AGO2 and DICER, but not TRBP2, proteins, to manage centrosomal homeostasis. In addition to TRBP2, endogenous UPF1 did not demonstrate AGO2-specific (co-)localization patterns at key mitotic structures, thereby indicating a non-canonical, RNAi-dependent, pathway that lacks TRBP2 (and UPF1), and primarily relies on AGO2 and DICER activity during mitosis. To experimentally validate the role of TRBP2 protein in centrosomal RNAi machinery, mouse embryonic fibroblasts (MEFs) derived from both control ($TRBP2^{+/+}$) and null ($TRBP2^{-/-}$) mice should be mechanistically exploited. Spatial transcriptomics-mediated profiling of the mRNA/siRNA species populating either $TRBP2^{+/+}$ or $TRBP2^{-/-}$ MEF-residing centrosomes in dividing/mitotic vs. interphase cells may indicate TRBP2-independent centrosome-specific RNAi machinery that functions non-canonically during mitosis. As *TARBP2* (encoding TRBP2 protein) homozygous null mice are characterized by lethal phenotype at the weaning stage (95-97), cells from $TRBP2^{-/-}$ adult mouse tissues cannot be attained. Furthermore, mice homozygous for a targeted *UPF1* null mutation ($UPF1^{-/-}$) are viable in the pre-implantation period, but embryos resorb in the early post-implantation period (95-97), thus complicating the acquisition, proliferation and maintenance of $UPF1^{-/-}$ cells from adult mouse tissues. To

overcome these limitations, the RNAi and clustered regularly interspaced short palindromic repeats/CRISPR-associated protein 9 gene expression-targeting technology can also be applied, although clonal variation in gene silencing efficiency, or negative selection (due to gene targeting-induced lethality) of the gene-targeted cells cannot be excluded, impeding reliable and comprehensive interpretation of the obtained data.

The centrosome/mitotic spindle/cytokinetic bridge pathway-specific RNAi machinery, due to its potential intrinsic instability, may be undetected during interphase, but structurally stabilized at mitosis, through its physical association with tubulin-containing microtubules. The mitotic microtubular network may serve as scaffold for biosynthesis, assembly, stabilization and function of the AGO2^{+}/DICER^{+}/TRBP2^{-}/UPF1^{-} machinery to exert non-canonical, RNAi-specific actions to control local homeostasis. Of note, our previous study (17) demonstrated that actin filaments do not control the AGO2 subcellular distribution, as cell exposure to cytochalasin D, a chemical compound that specifically targets actin dynamics, by disrupting actin (micro-)filaments and inhibiting actin polymerization, does not cause detectable changes in AGO2 typical distribution during mitosis, highlighting the mechanistic dependence of AGO2 localization and functionality on microtubule network stability and integrity.

Structural integrity of microtubule polymerization-derived cytoskeleton may enable non-canonical, RNAi-dependent pathways to act locally and control essential mitotic assemblies, such as the centrosome, mitotic spindle and the cytokinetic bridge. As demecolcine-induced disintegration of microtubular cytoskeleton causes the disappearance of AGO2-α-tubulin co-localization patterns, both at interphase and mitosis, and generation of aberrant centrosome number, geometry, topology and orientation does not alter the AGO2-α-tubulin co-localization immuno-profiling at the abnormal mitotic centrosomes and spindles (multi-polar spindles) during the cell cycle, the α-tubulin-derived cytoskeleton may serve an important role in AGO2-containing complexes, with the AGO2^{+}/DICER^{+}/TRBP2^{-}/UPF1^{-} apparatus potentially exploiting the microtubular cytoskeleton for its structural scaffolding and locality-dependent, RNAi-specific activity.

Altogether, the present study demonstrated that AGO2 is an essential regulator of the maintenance of mRNA/protein local homeostasis and may direct the formation of non-canonical, RNAi-dependent molecular machinery that controls the centrosome/mitotic spindle/cytokinetic bridge biosynthesis and functionality during mitosis of dividing (human) liver cells. Given its unique and atypical composition, and dependency on microtubule-network integrity, the AGO2^{+}/DICER^{+}/TRBP2^{-}/UPF1^{-}, non-canonical, RNAi-specific, (super-)complex may be a druggable molecular system. This may be spatially and temporally targeted, for the development of novel therapeutic strategies against diverse human pathologies, including liver cancer.

In conclusion, using advanced imaging and molecular bioinformatics, the present study demonstrated the compartmentalization of AGO2 protein in the centrosome, mitotic spindle and cytokinetic bridge assemblies of dividing human liver cells. The findings of the present study reveal novel, non-canonical, RNAi-dependent roles of AGO2 during mitosis in locality-specific control of sub-cellular homeostasis. Spatiotemporal (genetic or pharmaceutical) targeting of AGO2 may provide new therapeutic windows in human cancer.

Acknowledgements

The authors would like to thank Dr Athanassios D. Velentzas (Department of Biology, National and Kapodistrian University of Athens, Athens, Greece) for their advice.

Funding

The present study was supported by the Hellenic Foundation for Research and Innovation (Athens, Greece), under the '3rd Call for HFRI PhD Fellowships' [grant no. 6318 (06/05/2022-05/12/2024)].

Authors' contributions

EA and DS conceived the study, and constructed figures. ET, PK, KN, EV, OT, GV, EA and DS analyzed data. ET, PK, EA and DS performed experiments. ET, PK, KN, EV, OT, GV, EA and DS designed experiments. DS supervised the study and edited the manuscript. ET and DS wrote the manuscript. All authors have read and approved the final manuscript. ET and DS confirm the authenticity of all the raw data.

Ethics approval and consent to participate

Not applicable.

Patient consent for publication

Not applicable.

Competing interests

The authors declare that they have no competing interests.

References

1. Oliveto S, Mancino M, Manfrini N and Biffo S: Role of microRNAs in translation regulation and cancer. World J Biol Chem 8: 45-56, 2017.
2. Croce CM: Causes and consequences of microRNA dysregulation in cancer. Nat Rev Genet 10: 704-714, 2009.
3. Bartel DP: MicroRNAs: Target recognition and regulatory functions. Cell 136: 215-233, 2009.
4. Bartel DP: MicroRNAs: Genomics, biogenesis, mechanism, and function. Cell 116: 281-297, 2004.
5. Lagos-Quintana M, Rauhut R, Lendeckel W and Tuschl T: Identification of novel genes coding for small expressed RNAs. Science 294: 853-858, 2001.
6. Beermann J, Piccoli MT, Viereck J and Thum T: Non-coding RNAs in development and disease: Background, mechanisms, and therapeutic approaches. Physiol Rev 96: 1297-1325, 2016.
7. Clark BS and Blackshaw S: Long non-coding RNA-dependent transcriptional regulation in neuronal development and disease. Front Genet 5: 164, 2014.
8. Sayed D and Abdellatif M: MicroRNAs in development and disease. Physiol Rev 91: 827-887, 2011.
9. Quévillon Huberdeau M, Zeitler DM, Hauptmann J, Bruckmann A, Fressigné L, Danner J, Piquet S, Strieder N, Engelmann JC, Jannot G, *et al*: Phosphorylation of argonaute proteins affects mRNA binding and is essential for microRNA-guided gene silencing in vivo. EMBO J 36: 2088-2106, 2017.

10. Hutvagner G and Simard MJ: Argonaute proteins: Key players in RNA silencing. Nat Rev Mol Cell Biol 9: 22-32, 2008.
11. Meister G: Argonaute proteins: Functional insights and emerging roles. Nat Rev Genet 14: 447-459, 2013.
12. Nowak I and Sarshad AA: Argonaute proteins take center stage in cancers. Cancers (Basel) 13: 788, 2021.
13. Bartel DP: Metazoan MicroRNAs. Cell 173: 20-51, 2018.
14. Hutvágner G and Zamore PD: A microRNA in a multiple-turnover RNAi enzyme complex. Science 297: 2056-2060, 2002.
15. Zeng Y and Cullen BR: Sequence requirements for micro RNA processing and function in human cells. RNA 9: 112-123, 2003.
16. Doench JG, Petersen CP and Sharp PA: siRNAs can function as miRNAs. Genes Dev 17: 438-442, 2003.
17. Pantazopoulou VI, Delis AD, Georgiou S, Pagakis SN, Filippa V, Dragona E, Kloukina I, Chatzitheodoridis E, Trebicka J, Velentzas AD, *et al*: AGO2 localizes to cytokinetic protrusions in a p38-dependent manner and is needed for accurate cell division. Commun Biol 4: 726, 2021.
18. Li X, Wang X, Cheng Z and Zhu Q: AGO2 and its partners: A silencing complex, a chromatin modulator, and new features. Crit Rev Biochem Mol Biol 55: 33-53, 2020.
19. Carmell MA, Xuan Z, Zhang MQ and Hannon GJ: The argonaute family: Tentacles that reach into RNAi, developmental control, stem cell maintenance, and tumorigenesis. Genes Dev 16: 2733-2742, 2002.
20. Nakanishi K: Anatomy of four human argonaute proteins. Nucleic Acids Res 50: 6618-6638, 2022.
21. Song JJ, Smith SK, Hannon GJ and Joshua-Tor L: Crystal structure of argonaute and its implications for RISC slicer activity. Science 305: 1434-1437, 2004.
22. Yuan YR, Pei Y, Ma JB, Kuryavyi V, Zhadina M, Meister G, Chen HY, Dauter Z, Tuschl T and Patel DJ: Crystal structure of A. aeolicus argonaute, a site-specific DNA-guided endoribonuclease, provides insights into RISC-mediated mRNA cleavage. Mol Cell 19: 405-419, 2005.
23. Ma JB, Ye K and Patel DJ: Structural basis for overhang-specific small interfering RNA recognition by the PAZ domain. Nature 429: 318-322, 2004.
24. Ma JB, Yuan YR, Meister G, Pei Y, Tuschl T and Patel DJ: Structural basis for 5'-end-specific recognition of guide RNA by the A. fulgidus Piwi protein. Nature 434: 666-670, 2005.
25. Höck J and Meister G: The argonaute protein family. Genome Biol 9: 210, 2008.
26. Chu Y, Yokota S, Liu J, Kilikevicius A, Johnson KC and Corey DR: Argonaute binding within human nuclear RNA and its impact on alternative splicing. RNA 27: 991-1003, 2021.
27. Park MS, Sim G, Kehling AC and Nakanishi K: Human argonaute2 and argonaute3 are catalytically activated by different lengths of guide RNA. Proc Natl Acad Sci USA 117: 28576-28578, 2020.
28. Robb GB, Brown KM, Khurana J and Rana TM: Specific and potent RNAi in the nucleus of human cells. Nat Struct Mol Biol 12: 133-137, 2005.
29. Rüdel S, Flatley A, Weinmann L, Kremmer E and Meister G: A multifunctional human argonaute2-specific monoclonal antibody. RNA 14: 1244-1253, 2008.
30. Wu J, Yang J, Cho WC and Zheng Y: Argonaute proteins: Structural features, functions and emerging roles. J Adv Res 24: 317-324, 2020.
31. Ameyar-Zazoua M, Rachez C, Souidi M, Robin P, Fritsch L, Young R, Morozova N, Fenouil R, Descostes N, Andrau JC, *et al*: Argonaute proteins couple chromatin silencing to alternative splicing. Nat Struct Mol Biol 19: 998-1004, 2012.
32. Perron MP and Provost P: Protein components of the microRNA pathway and human diseases. Methods Mol Biol 487: 369-385, 2009.
33. Liu J, Carmell MA, Rivas FV, Marsden CG, Thomson JM, Song JJ, Hammond SM, Joshua-Tor L and Hannon GJ: Argonaute2 is the catalytic engine of mammalian RNAi. Science 305: 1437-1441, 2004.
34. Morita S, Horii T, Kimura M, Goto Y, Ochiya T and Hatada I: One argonaute family member, Eif2c2 (Ago2), is essential for development and appears not to be involved in DNA methylation. Genomics 89: 687-696, 2007.
35. O'Carroll D, Mecklenbrauker I, Das PP, Santana A, Koenig U, Enright AJ, Miska EA and Tarakhovsky A: A slicer-independent role for argonaute 2 in hematopoiesis and the microRNA pathway. Genes Dev 21: 1999-2004, 2007.
36. Schirle NT, Sheu-Gruttadauria J, Chandradoss SD, Joo C and MacRae IJ: Water-mediated recognition of t1-adenosine anchors argonaute2 to microRNA targets. Elife 4: e07646, 2015.
37. de Vries I, Kwakman T, Lu XJ, Hekkelman ML, Deshpande M, Velankar S, Perrakis A and Joosten RP: New restraints and validation approaches for nucleic acid structures in PDB-REDO. Acta Crystallogr D Struct Biol 77: 1127-1141, 2021.
38. Sastry GM, Adzhigirey M, Day T, Annabhimoju R and Sherman W: Protein and ligand preparation: Parameters, protocols, and influence on virtual screening enrichments. J Comput Aided Mol Des 27: 221-234, 2013.
39. Jones G, Jindal A, Ghani U, Kotelnikov S, Egbert M, Hashemi N, Vajda S, Padhorny D and Kozakov D: Elucidation of protein function using computational docking and hotspot analysis by ClusPro and FTMap. Acta Crystallogr D Struct Biol 78: 690-697, 2022.
40. Gowravaram M, Bonneau F, Kanaan J, Maciej VD, Fiorini F, Raj S, Croquette V, Le Hir H and Chakrabarti S: A conserved structural element in the RNA helicase UPF1 regulates its catalytic activity in an isoform-specific manner. Nucleic Acids Res 46: 2648-2659, 2018.
41. Kim J, Li CL, Chen X, Cui Y, Golebiowski FM, Wang H, Hanaoka F, Sugasawa K and Yang W: Lesion recognition by XPC, TFIIH and XPA in DNA excision repair. Nature 617: 170-175, 2023.
42. Theotoki EI, Kakoulidis P, Velentzas AD, Nikolakopoulos KS, Angelis NV, Tsitsilonis OE, Anastasiadou E and Stravopodis DJ: TRBP2, a major component of the RNAi machinery, is subjected to cell cycle-dependent regulation in human cancer cells of diverse tissue origin. Cancers (Basel) 16: 3701, 2024.
43. Li F, Li Y, Ye X, Gao H, Shi Z, Luo X, Rice LM and Yu H: Cryo-EM structure of VASH1-SVBP bound to microtubules. Elife 9: e58157, 2020.
44. Wieczorek M, Urnavicius L, Ti SC, Molloy KR, Chait BT and Kapoor TM: Asymmetric molecular architecture of the human γ-tubulin ring complex. Cell 180: 165-175.e16, 2020.
45. Rice LM, Montabana EA and Agard DA: The lattice as allosteric effector: Structural studies of alphabeta- and gamma-tubulin clarify the role of GTP in microtubule assembly. Proc Natl Acad Sci USA 105: 5378-5383, 2008.
46. Burley SK, Bhatt R, Bhikadiya C, Bi C, Biester A, Biswas P, Bittrich S, Blaumann S, Brown R, Chao H, *et al*: Updated resources for exploring experimentally-determined PDB structures and computed structure models at the RCSB protein data bank. Nucleic Acids Res 53 (D1): D564-D574, 2025.
47. Eastman P, Galvelis R, Peláez RP, Abreu CRA, Farr SE, Gallicchio E, Gorenko A, Henry MM, Hu F, Huang J, *et al*: OpenMM 8: Molecular dynamics simulation with machine learning potentials. J Phys Chem B 128: 109-116, 2024.
48. Jurrus E, Engel D, Star K, Monson K, Brandi J, Felberg LE, Brookes DH, Wilson L, Chen J, Liles K, *et al*: Improvements to the APBS biomolecular solvation software suite. Protein Sci 27: 112-128, 2018.
49. Lee YY, Lee H, Kim H, Kim VN and Roh SH: Structure of the human DICER-pre-miRNA complex in a dicing state. Nature 615: 331-338, 2023.
50. Arab SS and Dantism A: EasyModel: A user-friendly web-based interface based on MODELLER. Sci Rep 13: 17185, 2023.
51. Webb B and Sali A: Comparative protein structure modeling using MODELLER. Curr Protoc Bioinformatics 54: 5.6.1-5.6.37, 2016.
52. Deshmukh P, Markande S, Fandade V, Ramtirtha Y, Madhusudhan MS and Joseph J: The miRISC component AGO2 has multiple binding sites for Nup358 SUMO-interacting motif. Biochem Biophys Res Commun 556: 45-52, 2021.
53. Laskowski RA and Thornton JM: PDBsum extras: SARS-CoV-2 and AlphaFold models. Protein Sci 31: 283-289, 2022.
54. Honorato RV, Koukos PI, Jiménez-García B, Tsaregorodtsev A, Verlato M, Giachetti A, Rosato A and Bonvin AMJJ: Structural biology in the clouds: The WeNMR-EOSC ecosystem. Front Mol Biosci 8: 729513, 2021.
55. Abramson J, Adler J, Dunger J, Evans R, Green T, Pritzel A, Ronneberger O, Willmore L, Ballard AJ, Bambrick J, *et al*: Accurate structure prediction of biomolecular interactions with AlphaFold 3. Nature 630: 493-500, 2024.
56. UniProt Consortium: UniProt: The universal protein knowledgebase in 2025. Nucleic Acids Res 53 (D1): D609-D617, 2025.
57. Yamashita K, Wojdyr M, Long F, Nicholls RA and Murshudov GN: GEMMI and Servalcat restrain REFMAC5. Acta Crystallogr D Struct Biol 79: 368-373, 2023.
58. Humphrey W, Dalke A and Schulten K: VMD: Visual molecular dynamics. J Mol Graph 14: 33-38, 27-28, 1996.

59. Meng EC, Goddard TD, Pettersen EF, Couch GS, Pearson ZJ, Morris JH and Ferrin TE: UCSF ChimeraX: Tools for structure building and analysis. Protein Sci 32: e4792, 2023.
60. Orchard S, Ammari M, Aranda B, Breuza L, Briganti L, Broackes-Carter F, Campbell NH, Chavali G, Chen C, del-Toro N, *et al*: The MIntAct project-IntAct as a common curation platform for 11 molecular interaction databases. Nucleic Acids Res 42 (Database Issue): D358-D363, 2014.
61. Liu J, Valencia-Sanchez MA, Hannon GJ and Parker R: MicroRNA-dependent localization of targeted mRNAs to mammalian P-bodies. Nat Cell Biol 7: 719-723, 2005.
62. Salisbury JL, Suino KM, Busby R and Springett M: Centrin-2 is required for centriole duplication in mammalian cells. Curr Biol 12: 1287-1292, 2002.
63. Bettencourt-Dias M and Glover DM: Centrosome biogenesis and function: Centrosomics brings new understanding. Nat Rev Mol Cell Biol 8: 451-463, 2007.
64. Buhler M and Stolz A: Estrogens-origin of centrosome defects in human cancer? Cells 11: 432, 2022.
65. Moritz M, Braunfeld MB, Sedat JW, Alberts B and Agard DA: Microtubule nucleation by gamma-tubulin-containing rings in the centrosome. Nature 378: 638-640, 1995.
66. Pihan GA: Centrosome dysfunction contributes to chromosome instability, chromoanagenesis, and genome reprograming in cancer. Front Oncol 3: 277, 2013.
67. Dammermann A and Merdes A: Assembly of centrosomal proteins and microtubule organization depends on PCM-1. J Cell Biol 159: 255-266, 2002.
68. Hames RS, Crookes RE, Straatman KR, Merdes A, Hayes MJ, Faragher AJ and Fry AM: Dynamic recruitment of Nek2 kinase to the centrosome involves microtubules, PCM-1, and localized proteasomal degradation. Mol Biol Cell 16: 1711-1724, 2005.
69. Staszewski J, Lazarewicz N, Konczak J, Migdal I and Maciaszczyk-Dziubinska E: UPF1-From mRNA degradation to human disorders. Cells 12: 419, 2023.
70. Jin H, Suh MR, Han J, Yeom KH, Lee Y, Heo I, Ha M, Hyun S and Kim VN: Human UPF1 participates in small RNA-induced mRNA downregulation. Mol Cell Biol 29: 5789-5799, 2009.
71. Welte T, Goulois A, Stadler MB, Hess D, Soneson C, Neagu A, Azzi C, Wisser MJ, Seebacher J, Schmidt I, *et al*: Convergence of multiple RNA-silencing pathways on GW182/TNRC6. Mol Cell 83: 2478-2492.e8, 2023.
72. Fiorini F, Bagchi D, Le Hir H and Croquette V: Human Upf1 is a highly processive RNA helicase and translocase with RNP remodelling activities. Nat Commun 6: 7581, 2015.
73. Cerulo L, Pezzella N, Caruso FP, Parente P, Remo A, Giordano G, Forte N, Busselez J, Boschi F, Galiè M, *et al*: Single-cell proteo-genomic reveals a comprehensive map of centrosome-associated spliceosome components. iScience 26: 106602, 2023.
74. Wynn TA: Cellular and molecular mechanisms of fibrosis. J Pathol 214: 199-210, 2008.
75. Völler D, Linck L, Bruckmann A, Hauptmann J, Deutzmann R, Meister G and Bosserhoff AK: Argonaute family protein expression in normal tissue and cancer entities. PLoS One 11: e0161165, 2016.
76. Shen EZ, Chen H, Ozturk AR, Tu S, Shirayama M, Tang W, Ding YH, Dai SY, Weng Z and Mello CC: Identification of piRNA binding sites reveals the argonaute regulatory landscape of the C. elegans germline. Cell 172: 937-951.e18, 2018.
77. Sasaki T, Kuwata R, Hoshino K, Isawa H, Sawabe K and Kobayashi M: Argonaute 2 suppresses japanese encephalitis virus infection in aedes aegypti. Jpn J Infect Dis 70: 38-44, 2017.
78. Gou LT, Kang JY, Dai P, Wang X, Li F, Zhao S, Zhang M, Hua MM, Lu Y, Zhu Y, *et al*: Ubiquitination-deficient mutations in human Piwi cause male infertility by impairing histone-to-protamine exchange during spermiogenesis. Cell 169: 1090-1104.e13, 2017.
79. Lessel D, Zeitler DM, Reijnders MRF, Kazantsev A, Hassani Nia F, Bartholomäus A, Martens V, Bruckmann A, Graus V, McConkie-Rosell A, *et al*: Germline AGO2 mutations impair RNA interference and human neurological development. Nat Commun 11: 5797, 2020.
80. Detzer A, Engel C, Wünsche W and Sczakiel G: Cell stress is related to re-localization of argonaute 2 and to decreased RNA interference in human cells. Nucleic Acids Res 39: 2727-2741, 2011.
81. Leung AKL and Sharp PA: Quantifying Argonaute proteins in and out of GW/P-bodies: Implications in microRNA activities. Adv Exp Med Biol 768: 165-182, 2013.
82. Patel PH, Barbee SA and Blankenship JT: GW-bodies and P-bodies constitute two separate pools of sequestered non-translating RNAs. PLoS One 11: e0150291, 2016.
83. Karlikow M, Goic B, Mongelli V, Salles A, Schmitt C, Bonne I, Zurzolo C and Saleh MC: Drosophila cells use nanotube-like structures to transfer dsRNA and RNAi machinery between cells. Sci Rep 6: 27085, 2016.
84. Antoniou A, Baptista M, Carney N and Hanley JG: PICK1 links argonaute 2 to endosomes in neuronal dendrites and regulates miRNA activity. EMBO Rep 15: 548-556, 2014.
85. Zhang Y, Wang B, Chen X, Li W and Dong P: AGO2 involves the malignant phenotypes and FAK/PI3K/AKT signaling pathway in hypopharyngeal-derived FaDu cells. Oncotarget 8: 54735-54746, 2017.
86. Zhang K, Pomyen Y, Barry AE, Martin SP, Khatib S, Knight L, Forgues M, Dominguez DA, Parhar R, Shah AP, *et al*: AGO2 mediates MYC mRNA stability in hepatocellular carcinoma. Mol Cancer Res 18: 612-622, 2020.
87. Ye Z, Jin H and Qian Q: Argonaute 2: A novel rising star in cancer research. J Cancer 6: 877-882, 2015.
88. Li L, Yu C, Gao H and Li Y: Argonaute proteins: Potential biomarkers for human colon cancer. BMC Cancer 10: 38, 2010.
89. Vaksman O, Hetland TE, Trope CG, Reich R and Davidson B: Argonaute, Dicer, and Drosha are up-regulated along tumor progression in serous ovarian carcinoma. Hum Pathol 43: 2062-2069, 2012.
90. Gao CL, Sun R, Li DH and Gong F: PIWI-like protein 1 upregulation promotes gastric cancer invasion and metastasis. Onco Targets Ther 11: 8783-8789, 2018.
91. Feng B, Hu P, Lu SJ, Chen JB and Ge RL: Increased argonaute 2 expression in gliomas and its association with tumor progression and poor prognosis. Asian Pac J Cancer Prev 15: 4079-4083, 2014.
92. Shankar S, Pitchiaya S, Malik R, Kothari V, Hosono Y, Yocum AK, Gundlapalli H, White Y, Firestone A, Cao X, *et al*: KRAS engages AGO2 to enhance cellular transformation. Cell Rep 14: 1448-1461, 2016.
93. Zhang X, Graves P and Zeng Y: Overexpression of human argonaute2 inhibits cell and tumor growth. Biochim Biophys Acta 1830: 2553-2561, 2013.
94. Casey MC, Prakash A, Holian E, McGuire A, Kalinina O, Shalaby A, Curran C, Webber M, Callagy G, Bourke E, *et al*: Quantifying argonaute 2 (Ago2) expression to stratify breast cancer. BMC Cancer 19: 712, 2019.
95. Baldarelli RM, Smith CL, Ringwald M, Richardson JE and Bult CJ; Mouse Genome Informatics Group: Mouse genome informatics: An integrated knowledgebase system for the laboratory mouse. Genetics 227: iyae031, 2024.
96. Baldarelli RM, Smith CM, Finger JH, Hayamizu TF, McCright IJ, Xu J, Shaw DR, Beal JS, Blodgett O, Campbell J, *et al*: The mouse gene expression database (GXD): 2021 Update. Nucleic Acids Res 49 (D1): D924-D931, 2021.
97. Krupke DM, Begley DA, Sundberg JP, Richardson JE, Neuhauser SB and Bult CJ: The mouse tumor biology database: A comprehensive resource for mouse models of human cancer. Cancer Res 77: e67-e70, 2017.
98. Aizer A, Brody Y, Ler LW, Sonenberg N, Singer RH and Shav-Tal Y: The dynamics of mammalian P body transport, assembly, and disassembly in vivo. Mol Biol Cell 19: 4154-4166, 2008.
99. Moser JJ, Fritzler MJ and Rattner JB: Repression of GW/P body components and the RNAi microprocessor impacts primary ciliogenesis in human astrocytes. BMC Cell Biol 12: 37, 2011.
100. Alliegro MC, Alliegro MA and Palazzo RE: Centrosome-associated RNA in surf clam oocytes. Proc Natl Acad Sci USA 103: 9034-9038, 2006.
101. Chichinadze K, Lazarashvili A and Tkemaladze J: RNA in centrosomes: Structure and possible functions. Protoplasma 250: 397-405, 2013.
102. Alliegro MC and Alliegro MA: Centrosomal RNA correlates with intron-poor nuclear genes in Spisula oocytes. Proc Natl Acad Sci USA 105: 6993-6997, 2008.
103. Alliegro MC: The implications of centrosomal RNA. RNA Biol 5: 198-200, 2008.
104. Safieddine A, Coleno E, Salloum S, Imbert A, Traboulsi AM, Kwon OS, Lionneton F, Georget V, Robert MC, Gostan T, *et al*: A choreography of centrosomal mRNAs reveals a conserved localization mechanism involving active polysome transport. Nat Commun 12: 1352, 2021.

105. Fareh M, Yeom KH, Haagsma AC, Chauhan S, Heo I and Joo C: TRBP ensures efficient Dicer processing of precursor microRNA in RNA-crowded environments. Nat Commun 7: 13694, 2016.
106. Griffin KN, Walters BW, Li H, Wang H, Biancon G, Tebaldi T, Kaya CB, Kanyo J, Lam TT, Cox AL, *et al*: Widespread association of the argonaute protein AGO2 with meiotic chromatin suggests a distinct nuclear function in mammalian male reproduction. Genome Res 32: 1655-1668, 2022.
107. Atwood BL, Woolnough JL, Lefevre GM, Saint Just Ribeiro M, Felsenfeld G and Giles KE: Human ARGONAUTE 2 IS TETHERED TO RIBOSOmal RNA through MicroRNA interactions. J Biol Chem 291: 17919-17928, 2016.
108. Woolnough JL, Atwood BL and Giles KE: Argonaute 2 binds directly to tRNA genes and promotes gene repression in cis. Mol Cell Biol 35: 2278-2294, 2015.
109. Nazer E, Gómez Acuña L and Kornblihtt AR: Seeking the truth behind the myth: Argonaute tales from 'nuclearland'. Mol Cell 82: 503-513, 2022.
110. Li J, Kim T, Nutiu R, Ray D, Hughes TR and Zhang Z: Identifying mRNA sequence elements for target recognition by human argonaute proteins. Genome Res 24: 775-785, 2014.
111. Remo A, Li X, Schiebel E and Pancione M: The centrosome linker and its role in cancer and genetic disorders. Trends Mol Med 26: 380-393, 2020.